BEAM MODELS FOR THE HANGINGWALL OF DEEP, TABULAR EXCAVATIONS IN STRATIFIED ROCK

by

N A DE VILLIERS
BSc Eng (Civil)

University of Cape Town

A thesis submitted in partial fulfilment
of the requirements for the degree of Master of Science in Engineering

Department of Civil Engineering
University of Cape Town

February 1989

The University of Cape Town has been given the right to reproduce this thesis in whole or in part. Copyright is held by the author.

The copyright of this thesis vests in the author. No quotation from it or information derived from it is to be published without full acknowledgement of the source. The thesis is to be used for private study or non-commercial research purposes only.

Published by the University of Cape Town (UCT) in terms of the non-exclusive license granted to UCT by the author.

University of Cape Town

To Sally, for all your support and encouragement.

University of Cape Town

DECLARATION

This is to certify that the results, calculations and other work presented in this thesis are essentially my own work, and that no part of it has been submitted for a degree at any other university.

N A DE VILLIERS

February 1989

University of Cape Town

ACKNOWLEDGEMENTS

I wish to express my appreciation to the following people:

My supervisors, Professor J B Martin and Dr W W Bird for their guidance and encouragement.

The Chamber of Mines Research Organisation for the motivation for the study and financial assistance.

My postgraduate colleagues for their assistance.

Cheryl Wright for the typing of this manuscript.

The Foundation for Research and Development for their financial assistance.

University of Cape Town

SYNOPSIS

In the South African gold mining industry, mining is being conducted at depths of over 3 000 m below the surface. Severe fracturing and deformation of the rock occurs making it unlikely that stress analysis which treats the rock as a homogeneous elastic material will yield useful results about the behaviour around the excavation. The excavation, or stope, considered in this study is tabular. The stope occurs in stratified rock with bedding planes at approximately 1 m intervals. The height of the stope is about 1 m to 1.5 m and the length increases to over 100 m as mining progresses.

Shear fractures initiate ahead of the advancing stope, which together with the bedding planes separate the rock into distinct blocks of relatively intact material. The stratified nature of the material in the hangingwall (or roof) of the excavation, and the lack of cohesion in the bedding planes, suggests that separation occurs along the bedding planes, with each layer supporting its own weight. The lowest of these layers is referred to as the "hangingwall beam". Stope closure occurs at a distance of around 30 to 40 m behind the stope face.

This study focuses on the mechanics of the hangingwall beam with particular emphasis on the conditions for stable closure. In order to do this the stope is first analysed using a finite element model which treats the rock as a homogeneous elastic medium. By treating the hangingwall beam as a separate layer, 1 m thick, its behaviour is compared to that observed in practice. We find that the hangingwall beam does separate from the overlying rock, but that the axial stresses in the beam are tensile, thus contradicting the observed behaviour. In practice, compressive stresses exist in the hangingwall and footwall. It has been suggested that slip along the shear fractures generates the compressive stresses.

In constructing a mathematical model of the hangingwall beam we consider the beam to be made up of blocks 1 m deep and 1 m long. The blocks are treated as a homogeneous elastic material. The behaviour of such a beam is different from that of a fully homogeneous beam, because of the possibility of the formation of hinges.

University of Cape Town

By considering a range of simplified models of a beam composed of blocks, various questions regarding its stability can be addressed. These models consider beams of fixed span in which the weight is increased from zero to the full value. The largest unsupported halfspan which can be stably equilibrated is of the order of 31 m. The maximum stable deflection is 0.4 m, and therefore additional support is required to allow closure to occur statically. The nature of a single supporting spring that will let down the beam in a limiting, stable manner is identified. Once closure has taken place, the hangingwall beam is stable.

In order to obtain a realistic picture of the steady state configuration of the hangingwall beam, an analysis is performed which simulates the advancing stope face. The results show that the distance between the face and the point of closure is around 34 m which is in accord with the behaviour observed in practice.

The results have shown that the model which treats the hangingwall as a beam composed of blocks provides useful information about the mechanics of the hangingwall.

University of Cape Town

TABLE OF CONTENTS

University of Cape Town

University of Cape Town

University of Cape Town

CHAPTER 1

INTRODUCTION

Gold mining is presently being conducted at depths of over 3000 m below the surface. High stresses exist in the rock at such great depths and the rock is highly fractured resulting in large inelastic deformations. The mechanical behaviour of rock has been documented by various researchers (Jaeger and Cook (1969), Stagg and Zienkiewicz (1969), Jumikus (1979), Brady and Brown (1985)). Treating the rock as a homogeneous elastic medium does not yield useful information about the mechanical behaviour in the proximity of the excavation. The presence of joints influences the response of the rock and it is therefore important that a finite element analysis involving jointed rock masses should take into account the joints. Many researchers have studied this subject and various sophisticated joint elements have been formulated (Goodman, Taylor and Brekke (1968), Ladanyi and Archambault (1970), Zienkiewicz (1970), Goodman and Dubois (1972), Ghaboussi, et al (1973), Goodman and St John (1977), Goodman (1977), Wilson (1977), Roberds and Einstein (1978) Heuze and Barbour (1982), Desai, et al (1984), Beer (1985), Plesha (1986,1987)). In this study we shall make use of a simple finite element to model the fracture planes and parting planes.

The excavation or stope which shall be considered in this study is tabular, allowing the problem to be treated as plane strain. The stope occurs in stratified rock with bedding planes at approximately 1 m intervals. The height of the stope varies, but is generally between 1 m and 1.5 m. In this thesis a height of 1.5 m will be used. It will be assumed that the footwall (or floor) displaces upwards half the distance that the hangingwall (or roof) displaces downwards and hence closure of the stope occurs when the displacement of the hangingwall reaches 1 m. The length of the stope increases from 10 m to over 100 m as mining progresses. The fractures which occur in the rock around the stope play an important role in the deformation of the hangingwall and the footwall.

The stratified nature of the material in the hangingwall and the lack of cohesion in the parting planes suggests that separation will occur along the parting planes, with each layer supporting its own weight. The lowest of these layers will be referred to as the "hangingwall beam".

University of Cape Town

Stope closure occurs some distance behind the stope face. The hangingwall (or the hangingwall beam) deflects downward to meet the upward moving footwall. The distance between the point of closure and the face depends on the support provided, but is of the order of 30 to 40 m.

This study will focus on the underlying mechanics of the hangingwall beam, with particular emphasis on the role of the compressive axial force and the conditions for stable closure. In order to do so, the stope geometry is reviewed to investigate the role of the fractures and deformations in the mechanics of the hangingwall beam. The nature of the fracturing and the possible causes are discussed, as well as the subsequent deformations which occur in the proximity of the excavation.

An elastic finite element analysis of the excavation is presented in order to establish the behaviour of the hangingwall under these conditions. Two cases are studied. In the first case the rock is treated as a homogeneous elastic mass. In the second case the hangingwall is modelled as a separate layer, 1 m deep, in order to determine whether separation occurs and to what extent it occurs. The finite element code ABAQUS is used for the analyses.

In constructing a mathematical model of the hangingwall beam, it is important to consider the existence of the near vertical shear fractures which occur at approximately 1 m intervals. This suggests that the beam should be conceived as made up of blocks, approximately 1 m deep by 1 m long. Treating the blocks as homogeneous elastic material, we construct a simple model which allows us to focus on the most important features of the mechanical behaviour. The role of the compressive axial force in the behaviour of a beam made up of discrete blocks is studied. The features of the behaviour are identified and the questions which arise are addressed by considering a range of simplified models.

In practice, the point of closure of the excavation advances as the face advances. This suggests a "steady state", in which the hangingwall beam has a configuration which remains the same but moves as the face advances. A numerical model in which the face advances is relatively complex, and we shall concentrate initially on the analysis of stopes of fixed span in which the weight of the hangingwall beam is gradually increased from zero to its full

University of Cape Town

value. The object is to gain insight into the essential features of the problem, rather than to provide specific numerical results for particular cases.

Aspects of the behaviour of the hangingwall beam that are addressed in the initial analysis are: the limiting unsupported span, the conditions for safe closure, and the stability of the beam after closure has taken place. The simple conceptual models are used to illustrate the basic mechanics of the hangingwall beam.

The "steady state" configuration of the hangingwall beam is investigated by considering a finite element model of a stope in which the face advances with mining. We shall consider a model in which closure has already occurred because of the numerical difficulty associated with modelling the point at which closure takes place. Such a model provides a realistic loading procedure of the hangingwall beam, therefore it should give insight into the nature of the steady state configuration.

University of Cape Town

CHAPTER 2

REVIEW OF THE STOPE GEOMETRY

A study of the fracture pattern and the deformations which occur in the proximity of the stope is important in that it provides insight into the mechanisms which are active in supporting the hangingwall. This chapter describes the predominant fracture systems formed around deep-level stopes and the various modes of deformation observed.

In order to establish the extent of the fractured zone and the distribution and nature of the fracturing within that zone, detailed mapping in the stopes and observation of fractures in diamond drilled holes has been carried out (Adams et al (1981), Joughin and Jager (1984)). This work showed that there were certain common features in the pattern of fracturing as observed in various locations. A typical pattern, believed to be representative of most stopes, has been presented by Brummer and Crook (1985), Herrmann (1987) and Brummer (1987).

The deformation of the rock mass in the immediate vicinity of the stope face was investigated by means of various devices, some of which were designed specifically for this purpose. The essential modes of deformation have been identified by various researchers (Brummer (1985,1987), Herrmann (1987)).

University of Cape Town

2.1 PATTERN OF FRACTURING

The important features of the fracture pattern around a deep excavation are shown in Figure 2.1. The fractures can be divided into three categories :

(i) primary or shear fractures;
(ii) secondary or extension fractures;
(iii) horizontal parting planes.

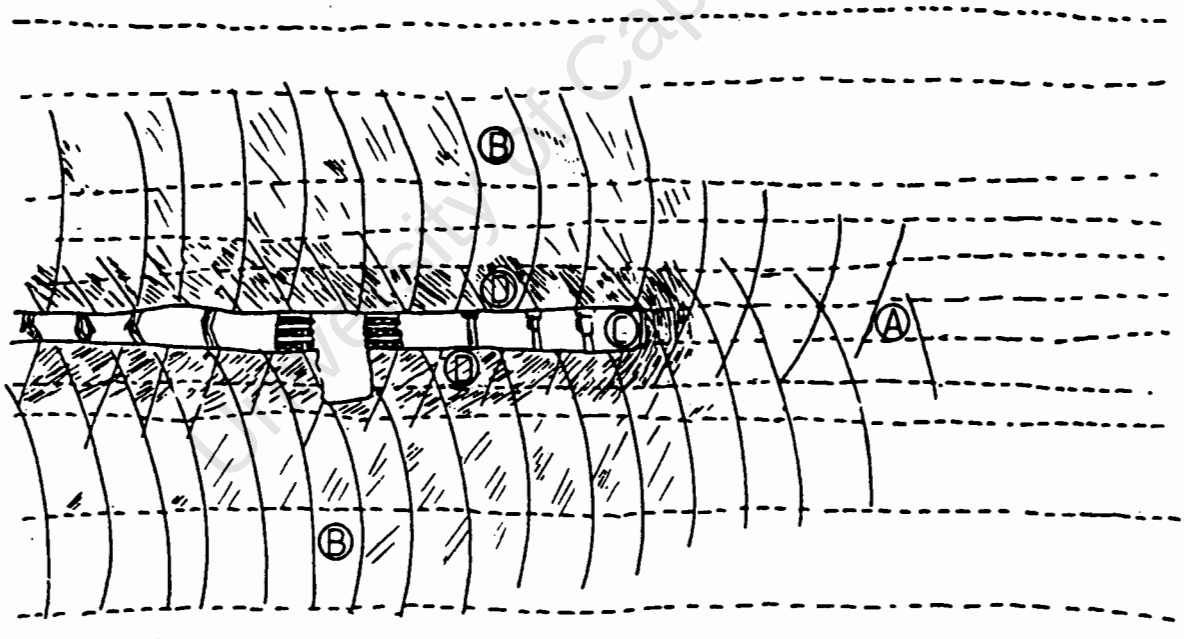

University of Cape Town

Figure 2.1 : Fracture pattern near a typical stope
(after Brummer (1987))

These are described below.

2.1.1 Shear fractures

Shear fractures occur in the rock surrounding deep level excavations. They are not found in the proximity of excavations at shallow levels, indicating that they are associated with highly stressed rock. They initiate at distances between 6 m and 8 m ahead of the advancing stope face at A in Figure 2.1 and separate the rock into blocks of relatively intact material. The shear fractures are more or less parallel to the stope face and occur at a fairly regular spacing of about 1 m. These shear fractures, which penetrate all rock strata, usually occur in conjugate pairs. Those in the hangingwall dip towards the excavation at about 60° to 80° and those in the footwall dipping away from it at the same angle. The fracture planes range in width from 5 mm to over 200 mm and contain a white powdery material.

The shear fractures in the regions indicated by B have already formed. They have negligible cohesion along the fractures, allowing movement to occur along the fracture planes. They curve back towards the excavation at depths of the order of 7 m into the hanging- and footwalls and display a decreasing amount of shear displacement with distance from the excavation.

2.1.2 Extension fractures

Extension fractures form a small distance ahead of the stope face as indicated by C in Figure 2.1 where conditions of low lateral confinement occur. They initiate after the shear fractures have formed and their formation is probably due to a lowering of the minor principal stress to the extent that the rock fractures in an almost uniaxial stress field. The extension fractures are parallel to the stope face immediately ahead of it and are inclined at between 80° and 120° to the horizontal in the hangingwall and footwall at D in Figure 2.1. They are of the order of 1 mm wide and occur at spacings of between 5 mm and 30 mm. There is no shear displacement across the fractures.

University of Cape Town

The fractures are truncated by parting planes and do not extend as far into the surrounding strata as do shear fractures. They may be observed in shallow mining operations where overburden stresses are lower and lateral confinement is less effective. Shear fractures would not occur under such conditions.

2.1.3 Parting planes

The rock surrounding the gold mine stopes generally occurs in near horizontal layers between 1 m and 1.5 m in width, separated by shaley layers or parting planes. These planes average 3 cm to 5 cm in width. They have a low frictional resistance and are weaker than the surrounding quartzites, thus allowing relative horizontal movements to occur.

2.2 DEFORMATIONS AT THE EDGES OF THE EXCAVATION

Large inelastic deformations which cannot be predicted by elastic analysis of the stope occur in the proximity of the excavation. They result from the fractures which have been described in the previous section. The inelastic deformations which occur are as follows :

(i) Sliding on shear planes
(ii) Displacement towards the stope and dilation
(iii) Sliding on parting planes
(iv) Stope closure.

The deformations are illustrated in Figure 2.2 and described in the sections which follow.

2.2.1 Sliding on shear planes

Stable shear failure occurs ahead of the stope, resulting in deformations along shear fractures. These inelastic displacements can be extremely large. It has been noted that the shear planes form in response to a high vertical stress. This permits the rock to compress vertically, resulting in horizontal expansion towards the mined out area.

University of Cape Town

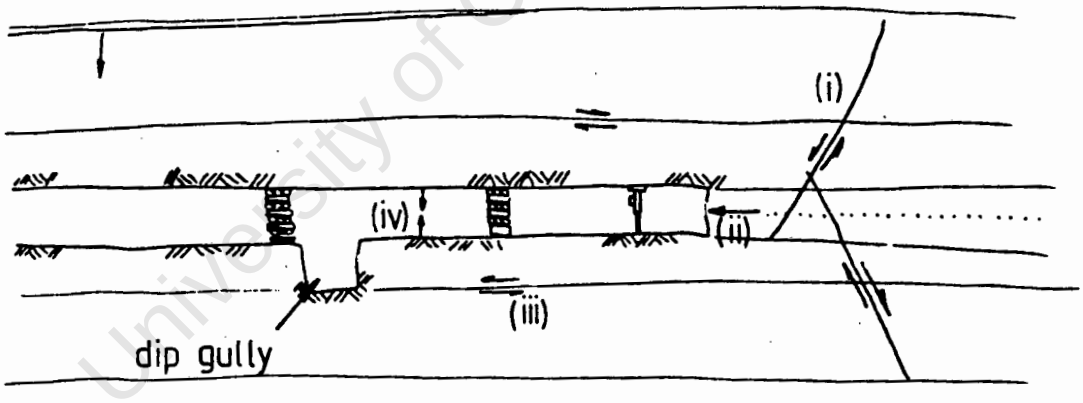

University of Cape Town

Figure 2.2 : Deformations around a typical stope
(after Brummer (1987))

2.2.2 Displacement towards the stope and dilation

Researchers have shown that a region of horizontally dilating rock, in some cases as deep as 10 m, exists ahead of the advancing stope face. This region advances with the face. The incidence of dilation corresponds to the region of fractured rock ahead of the stope, thus supporting the idea that slip on the shear fractures produces the dilation. The high vertical stresses developed ahead of the stope face compress the fractured rock producing further dilation of the rock towards the excavation.

2.2.3 Sliding on parting planes

Slip displacements commonly occur near the face on the horizontal parting planes in the host rock. Dip gulleys play an important role in facilitating horizontal movement of the footwall layers of rock. With the presence of a dip gulley, large horizontal displacements of the footwall are observed. When no dip gulley is present, the footwall is observed to buckle upward in response to large horizontal stresses. The slip along the shear fractures and subsequent dilation ahead of the stope face generates these horizontal compressive stresses in the hangingwall and footwall strata.

It has been found that slip occurs along several parting planes above the hangingwall and below the footwall. This leads to the notion that an "effective stope width" exists which is considerably wider than the stope itself. It includes rock in the hangingwall and footwall and is bounded by the parting planes along which significant slip occurs. The stratified nature of the material in the hangingwall, and the lack of cohesion in the parting planes suggest that separation will occur along the parting planes with each layer supporting its own weight. The lowest of these layers will be referred to as the "hangingwall beam".

University of Cape Town

2.2.4 Stope closure

Stope closure occurs some distance behind the stope face. The hangingwall (or the hangingwall beam) deflects downward to meet the upward moving footwall. The distance between the point of closure and the face depends on the support provided, but is of the order of 30 to 40 m. Closure occurs more rapidly than predicted by elastic models. This is attributed to the inelastic deformation which occurs ahead of the stope face and the separation which occurs between the layers of rock in the hangingwall.

University of Cape Town

CHAPTER 3

ELASTIC ANALYSIS OF A TYPICAL STOPE

3.1 INTRODUCTION

An idealised layout of a stope is shown in Figure 3.1. The span to height ratio of the stope is 100/1 and the stope occurs at a depth of over 2 000 m in sedimentary layers of rock. The stope is modelled using finite element analysis to determine the state of stress and deformation which occurs in the proximity of the excavation. The finite element method has been well documented by various researchers (Zienkiewicz (1971), Cooke (1972), Bathe (1982)).

The stope is tabular, allowing the analysis to be carried out in two dimensions with the material acting in plane strain. Symmetry about both the horizontal and the vertical axes can be assumed due to the great depth of the stope. As a result only one quarter of the stope need be modelled. The analysis uses material with an elastic response for the rock with Young's modulus and Poisson's ratio 70 GPa and 0.2 respectively. The selfweight of the rock is assumed to be 27 kN/m^3 and hence the vertical in-situ stress is 60 MPa at a depth of 2 225 m. Assuming plane strain with a Poisson's ratio of 0.2, and further assuming that there are no tectonic stresses present, the horizontal in-situ stress is 15 MPa.

It is relatively complex to simulate the advancing face and therefore it is assumed that the entire stope is mined out at the same time. The mining process is achieved in two loading steps :

(i) An initial stress field of 60 MPa vertically and 15 MPa horizontally is applied throughout the model. Pressures of 60 MPa and 15 MPa respectively are applied to the hangingwall and face of the stope, as shown in Figure 3.2, to simulate the

University of Cape Town

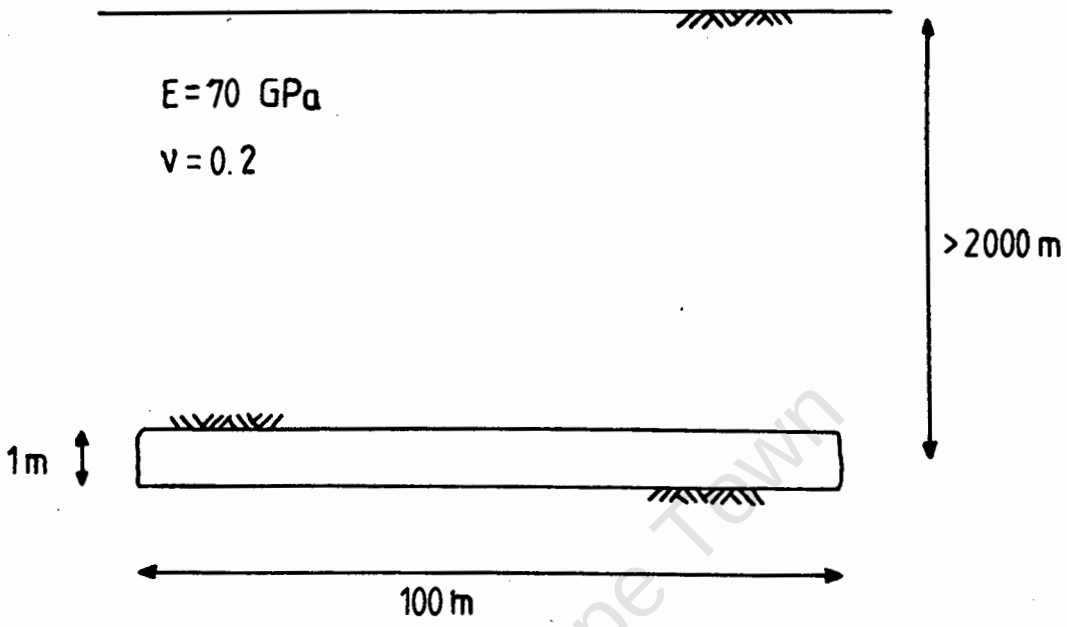

Figure 3.1 : Typical stope layout

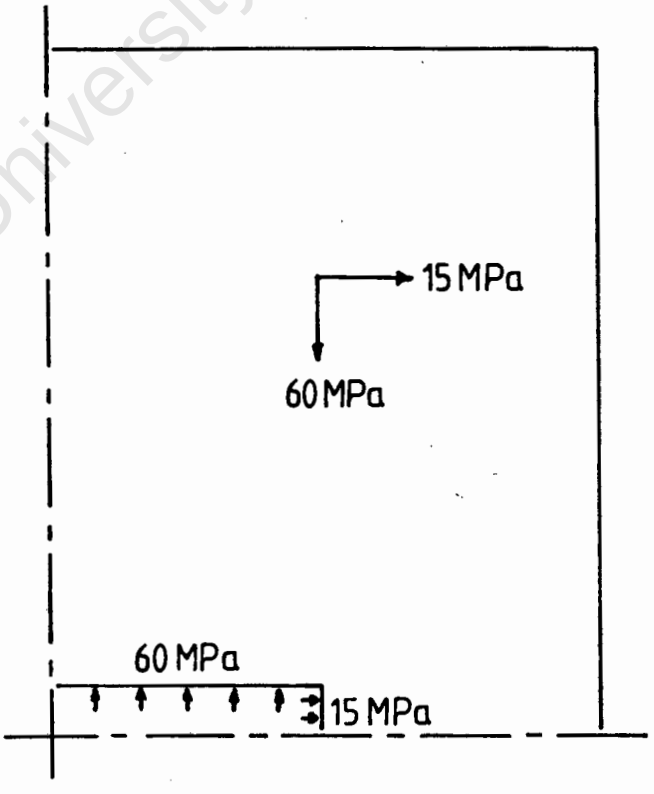

Figure 3.2 : Loading on the stope

University of Cape Town

stope prior to mining. A time step is allowed in order to obtain initial equilibrium.

(ii) The next step is to reduce to zero the pressure applied to the hangingwall and face of the stope to simulate the mining of the stope.

3.2 MESH STUDY

In order to model the stope accurately, the finite element mesh should extend to the surface and to infinite depth. Owing to the great depth of the stope (2 225 m), it would be costly and time consuming to do this. It is therefore either necessary to curtail the mesh at some distance above the stope or to make use of infinite elements. By using symmetry about the horizontal axis it is not necessary to include in the model the rock which occurs below the stope.

The finite element codes NOSTRUM and ABAQUS were used to do the analysis. NOSTRUM has infinite elements in its element library but the version we used had no interface or joint elements. ABAQUS (Hibbitt, Karlsson and Sorensen (1987)), on the other hand, has interface elements, but no infinite elements. It was necessary to use ABAQUS so that joints could be modelled using interface elements.

A mesh study was carried out to determine the extent of the mesh required to provide reasonably accurate results. NOSTRUM was used for an analysis which included infinite elements to provide a basis for comparison. Using ABAQUS, the stope was modelled with the finite element mesh extending a variable distance above the excavation.

The vertical displacement at the centre of the hangingwall is used as a measure of the accuracy of the results obtained with different finite element meshes. By plotting the displacement as a function of the height of the mesh, we can easily determine the mesh height required to yield sufficiently accurate results.

University of Cape Town

3.2.1 Infinite Element Model

The model in Figure 3.3 is used for this analysis. It consists of 112 eight-noded finite elements and 14 five-noded infinite elements. The analysis makes use of a relatively coarse mesh because of the limitation on the number of nodes imposed by the particular version of NOSTRUM.

The vertical displacement of the hangingwall is plotted in Figure 3.4. The vertical displacement at the centre of the hangingwall is 0.079 m.

3.2.2 Finite Element Model

The model used in this analysis consists of eight-noded serendipity elements extending 50 m horizontally ahead of the stope face and a vertical distance h metres above the hangingwall. Figure 3.5 shows the model used.

The model was analysed for different heights of the mesh above the hangingwall. Values of h varied between 50 m and 325 m. The vertical displacement of the centre of the hangingwall is plotted in Figure 3.6 for different values of the mesh height.

3.2.3 Discussion of Results

The results of the analysis using the finite element model indicate that the central vertical displacement converges to a maximum of approximately 0.080 m as the mesh height is increased. The value of the displacement using a mesh height of 325 m is 0.079 m. This corresponds to the value obtained using the infinite element model. Based on these results, the model provides sufficiently accurate results for a mesh height of 325 m.

University of Cape Town

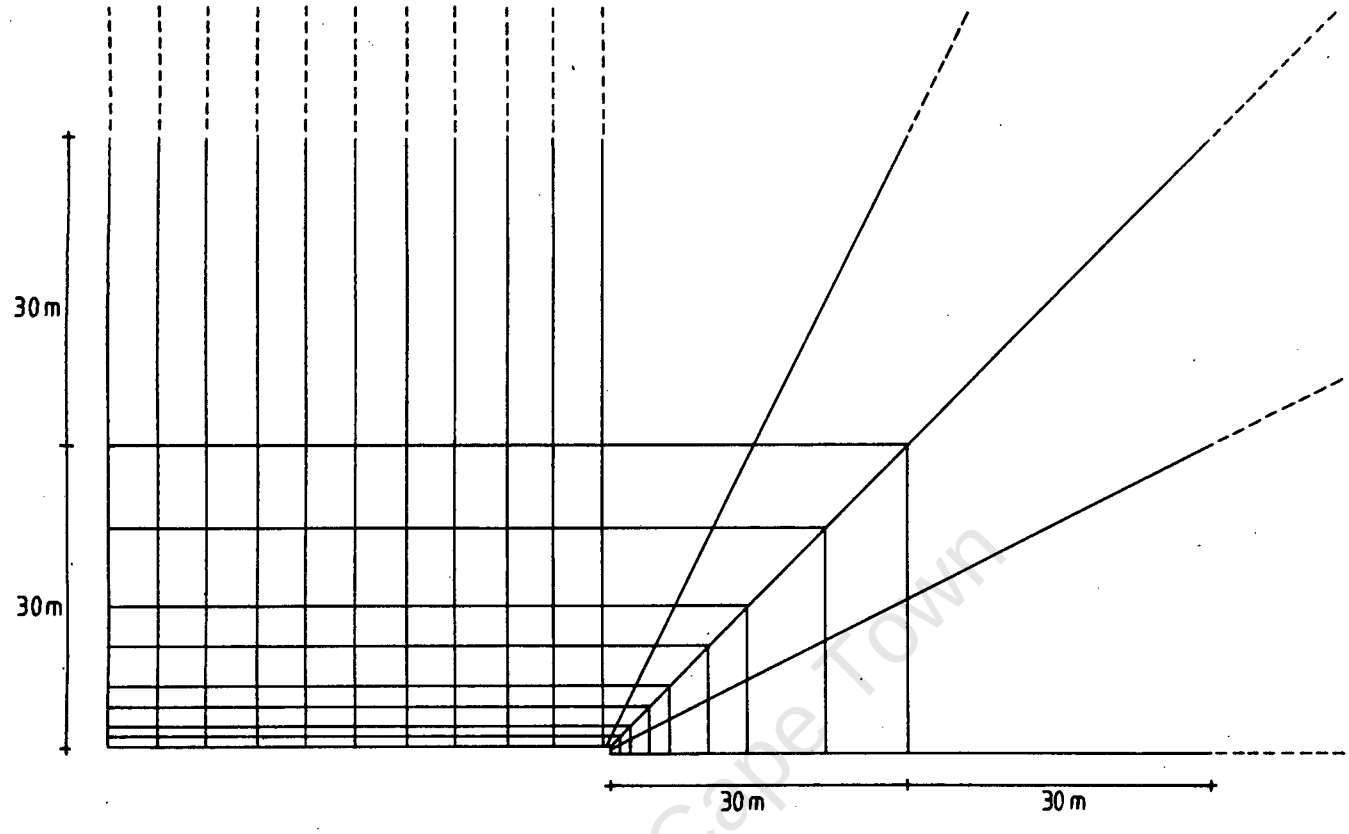

Figure 3.3 : Infinite element model

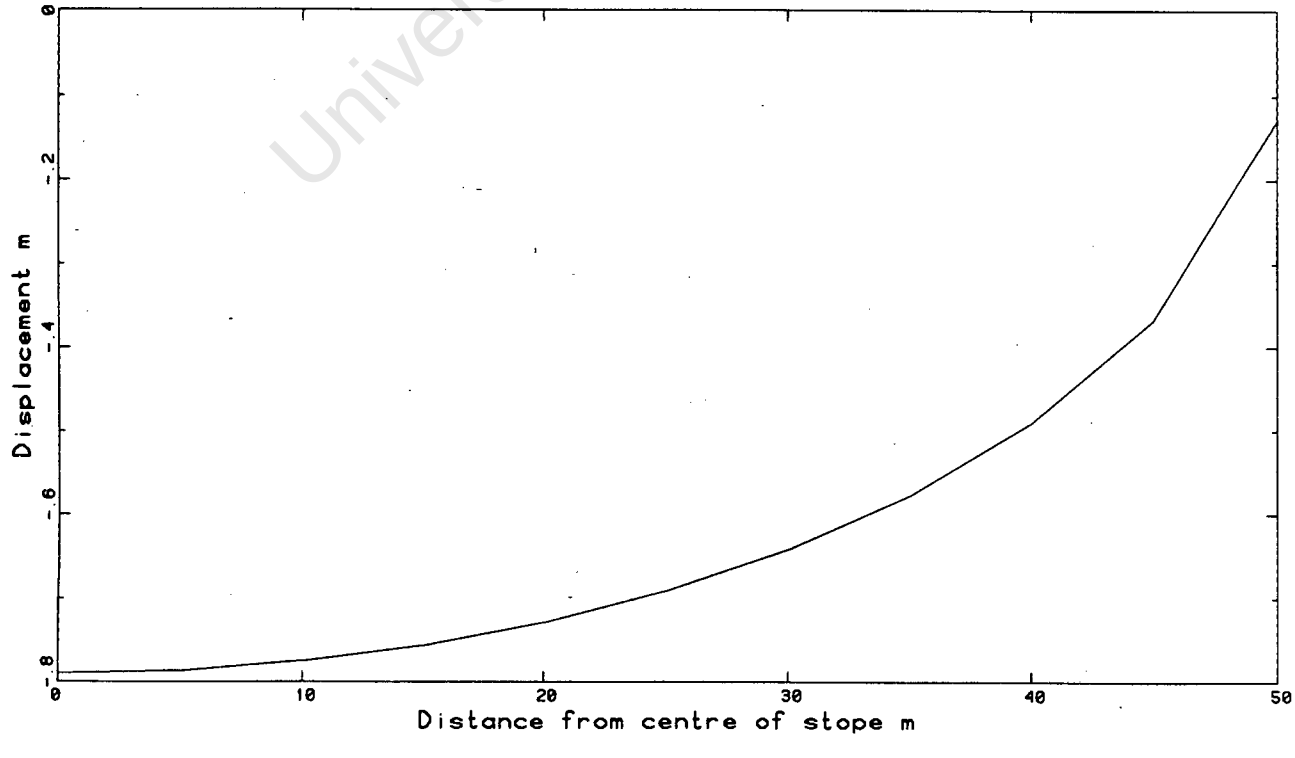

Figure 3.4 : Vertical displacement of the hangingwall for the infinite element model

University of Cape Town

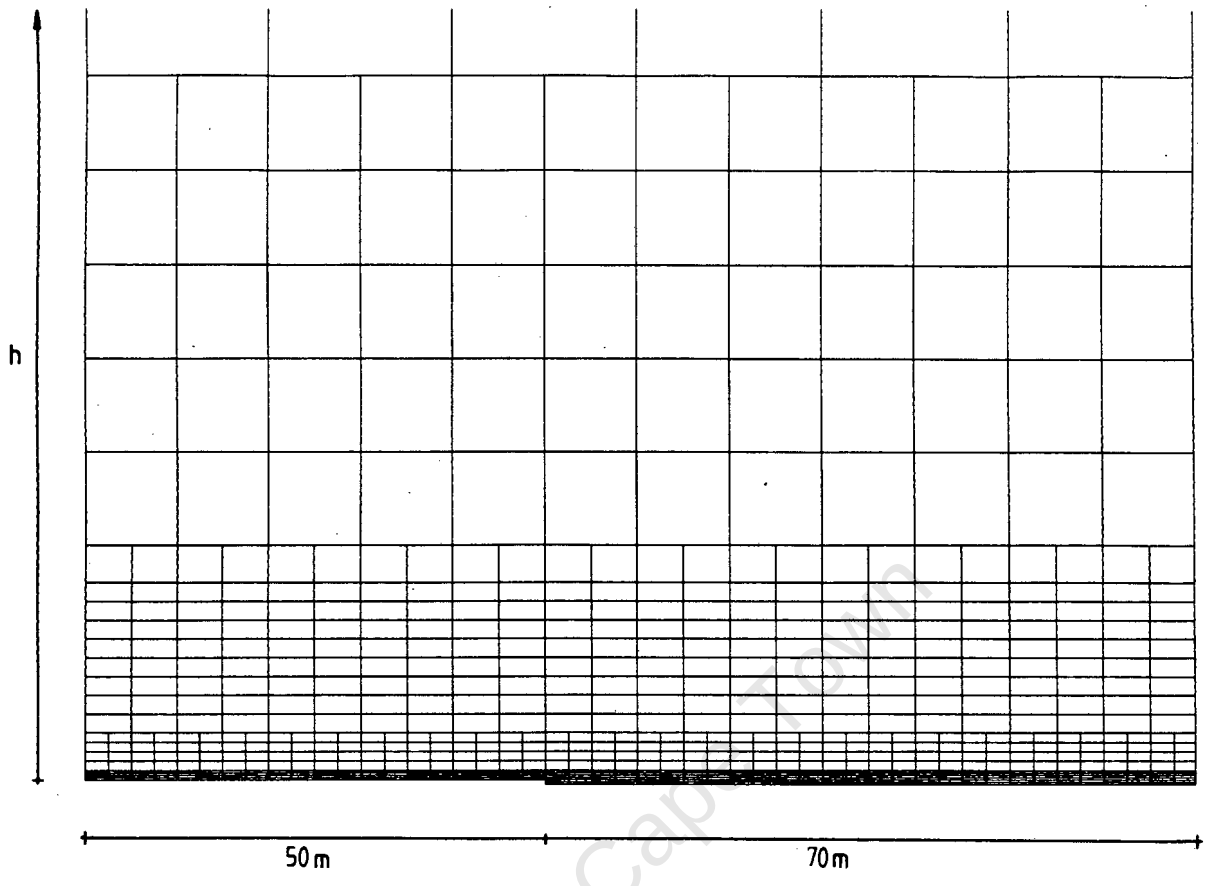

Figure 3.5 : Finite element model for the mesh study

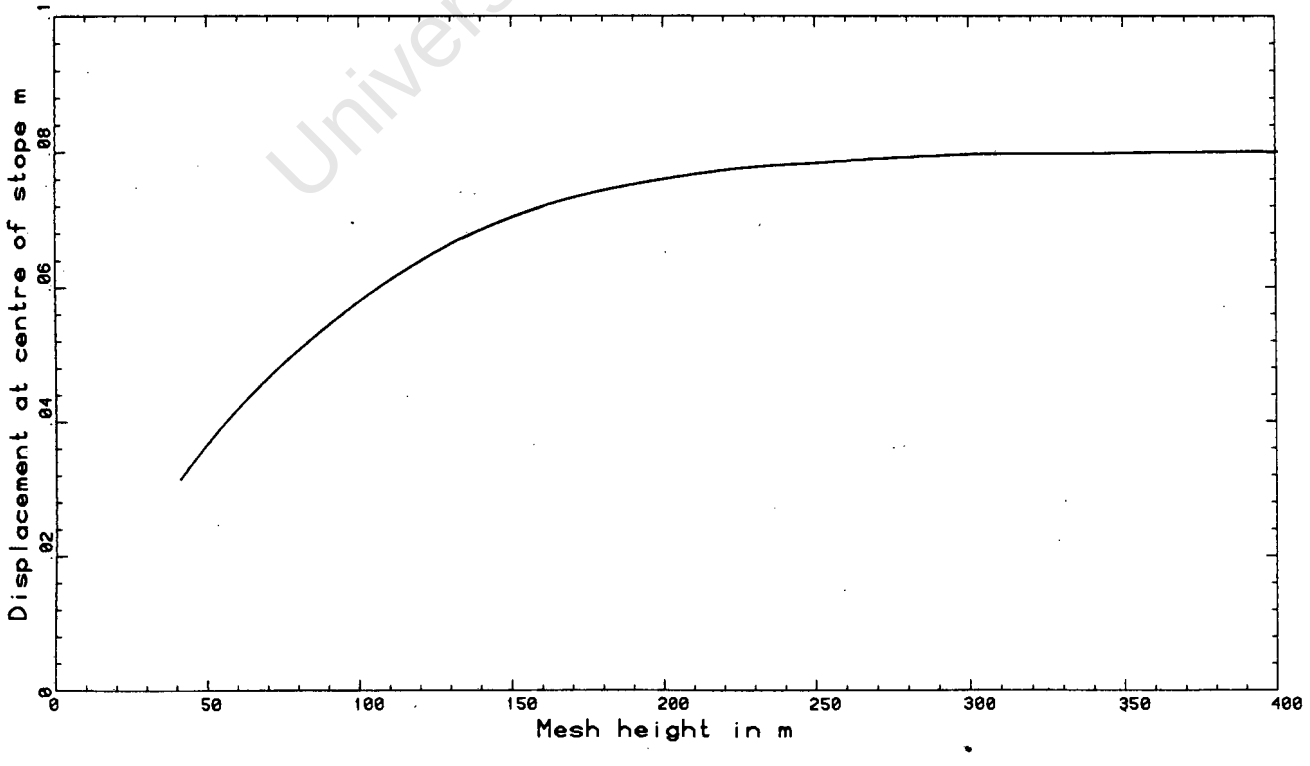

Figure 3.6 : Displacement vs mesh height

University of Cape Town

3.3 ANALYSIS OF THE EXCAVATION

The excavation was modelled using the finite element mesh in Figure 3.7 to establish the behaviour of the hangingwall under elastic conditions. Two cases were analysed. First, the case of a homogeneous, elastic rock mass was modelled to determine the state of stress and the displacements around the excavation. Second, the excavation was modelled with the hangingwall beam acting as a separate layer, 1 m deep, in order to determine the effect on the behaviour of the excavation. Nonlinear geometric effects were neglected in these analyses.

3.3.1 Homogeneous Model

Assuming the rock to be a homogeneous, elastic mass having a Young's Modulus and Poisson's Ratio of 70 GPa and 0.2 respectively, the excavation was modelled using the finite element mesh in Figure 3.7. The vertical displacement of the hangingwall is shown in Figure 3.8. This is much less than the observed deflection of the hangingwall. Horizontal tensile stresses are predicted in the hangingwall, contradicting the compressive stresses measured in practice. Figure 3.9 shows a plot of shear stresses along lines above the excavation. Very high shear stresses are predicted near the stope face, corresponding to the severely fractured zone observed in the field.

3.3.2 Layered Model

This analysis used the same finite element model as the homogeneous case, but the hangingwall beam is modelled as a separate layer, 1 m thick, having the same properties as the surrounding rock. Interface elements were used to model the joints between the rock layers.

The results of a small displacement analysis show that the hangingwall beam separates almost entirely from the overlying

University of Cape Town

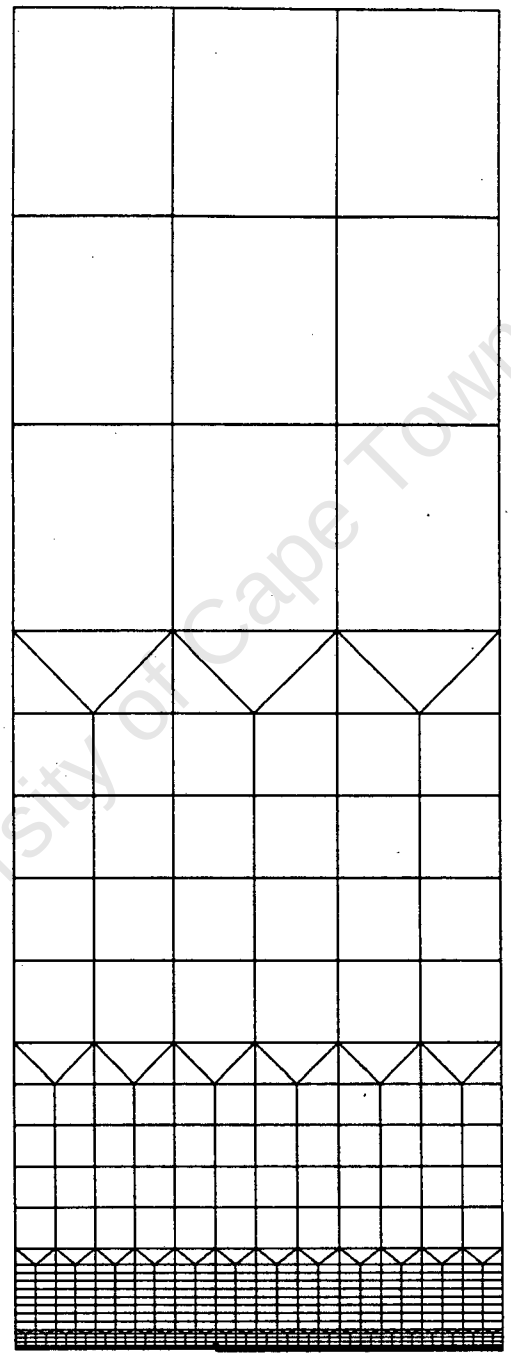

Figure 3.7 : Finite element mesh for homogeneous and layered model

University of Cape Town

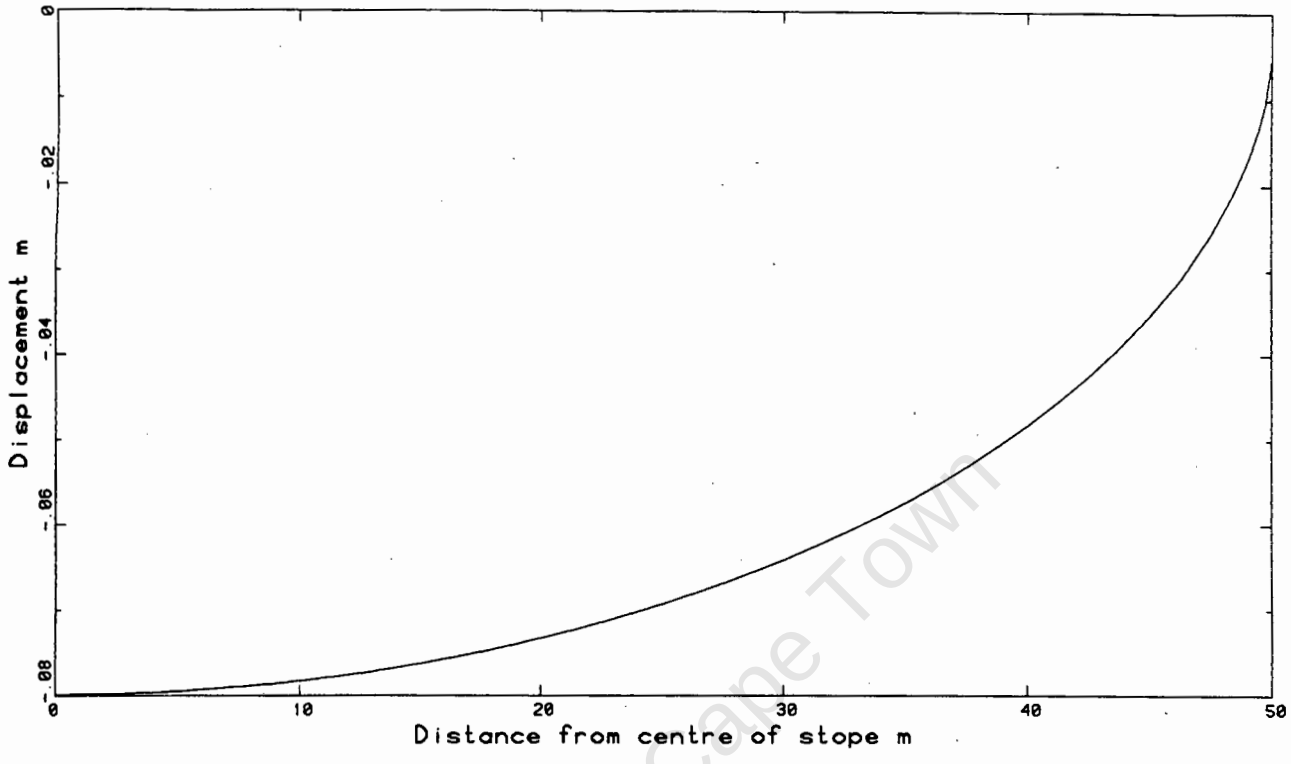

Figure 3.8 : Vertical displacement of the hangingwall for homogeneous model

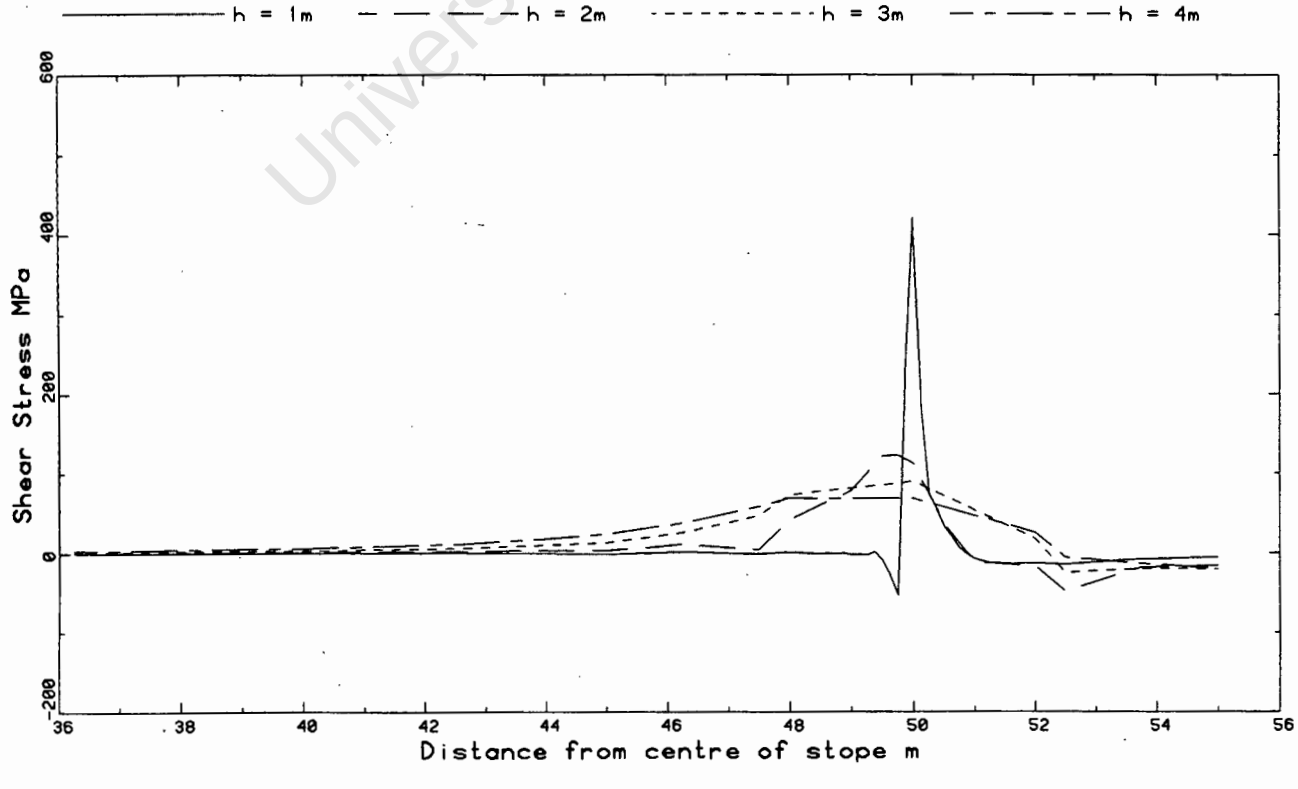

Figure 3.9 : Shear stresses at various heights above the stope

University of Cape Town

rock. The displaced stope is shown in Figure 3.10. The central deflection of the hangingwall is 1.204 m, indicating that closure of the excavation would have taken place in the central region.

The horizontal stresses at the centre of the hangingwall are shown in Figure 3.11. These stresses correspond to a uniform axial tension of 35 MPa and bending stresses corresponding to a transverse load of 27 kN/m, assuming a fully fixed beam. This implies that the hangingwall is acting as a fully fixed beam subjected to its self-weight and an axial tension of 35 000 kN.

These results suggest that separation occurs between the hangingwall beam and the overlying rock. This confirms that the hangingwall can be considered as a separate beam. This analysis predicts tensile stresses in the hangingwall which contradict the compressive stresses observed in practice. These results have been obtained for a stope of length 100 m. It is anticipated that the axial stresses are influenced by the length and that the tensile stresses would be smaller for stopes with shorter spans.

University of Cape Town

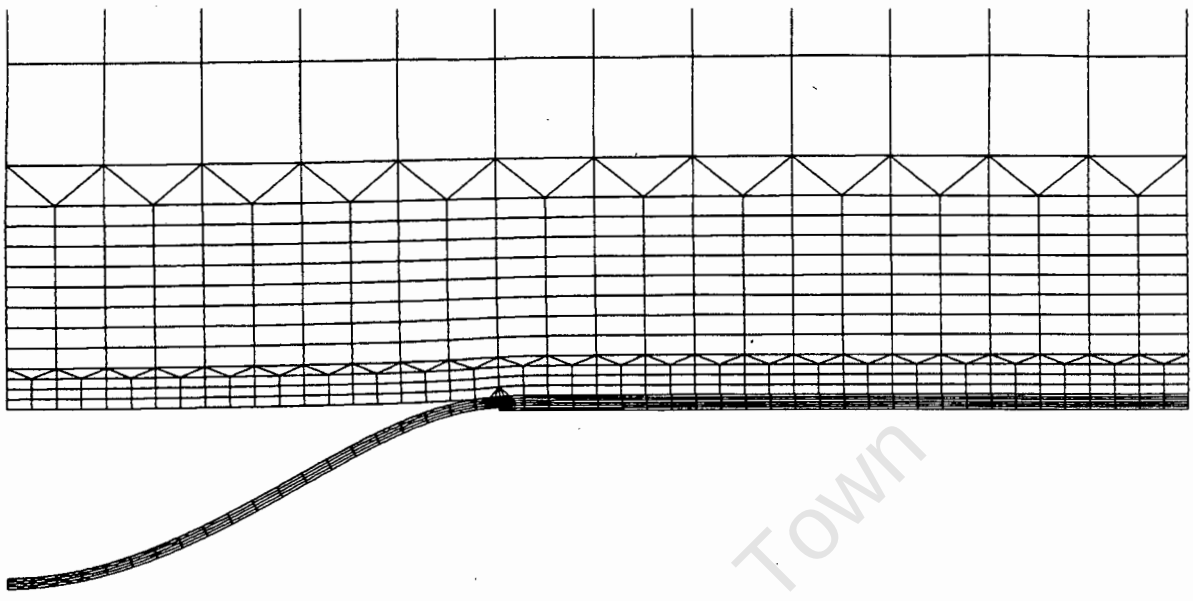

Figure 3.10 : Displaced shape of layered model
The displacements are not to scale

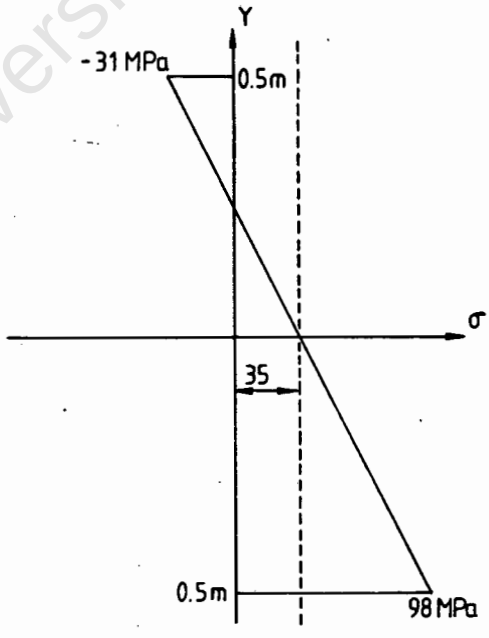

Figure 3.11 : Horizontal stresses at midspan of the hangingwall beam
Tension is positive

University of Cape Town

CHAPTER 4

MATHEMATICAL MODEL OF THE HANGINGWALL BEAM

The results from the elastic analysis indicate that it is not sufficient to regard the rock as a homogeneous mass, since they contradict the behaviour observed in practice. The fractured nature of the rock surrounding the excavation is not accounted for in a homogeneous elastic model, although it is important in determining the behaviour of the hangingwall beam. The elastic analysis also confirmed the suggestion that the hangingwall beam behaves as a seperate layer acting under its own weight. Previous researchers have described some aspects of the behaviour of such a beam (Evans (1941), Brady and Brown (1985)).

A model of the hangingwall beam is proposed which takes into account the fractured nature of the rock. The essential features are discussed, particularly the role of the compressive forces in maintaining equilibrium. Important aspects of the behaviour are described.

4.1 BASIS OF THE MATHEMATICAL MODEL

In constructing a realistic model of the hangingwall beam we shall take as an important feature the existence of the near-vertical shear fractures which originally form ahead of the stope face. This suggests that the beam should be considered as made up of blocks, approximately 1 m deep and 1 m long, as shown in Figure 4.1. In this model we shall idealise the situation by ignoring the extension fractures within the blocks, treating each block as homogeneous and elastic. It will be assumed that there is no cohesion across the vertical fractures, allowing separation to occur between adjacent blocks. This is an idealised model, but it permits us to focus on some of the most important features of the mechanical behaviour.

University of Cape Town

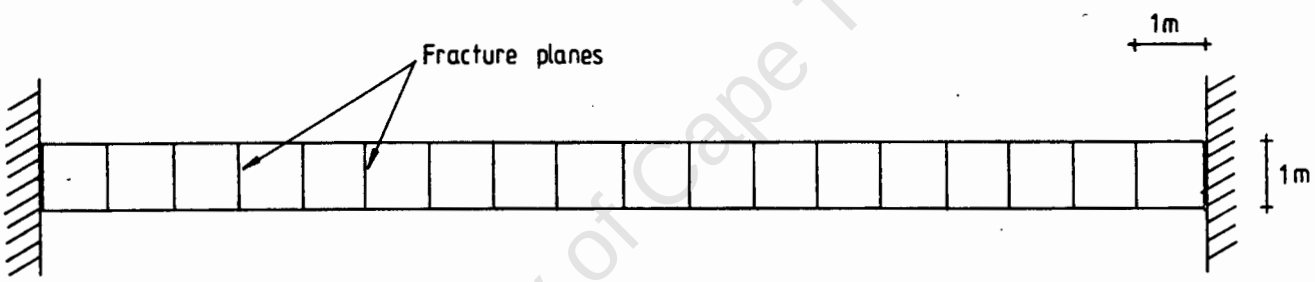

University of Cape Town

Figure 4.1 : Model of the hangingwall beam

The existence of vertical fractures leads to behaviour which is different from that of a fully homogeneous beam. This is so because of the possibility of masonry type hinges where there is separation on the tension side of the interfaces between adjacent blocks at points of large bending moment. When second order geometric effects are taken into account, the masonry hinges will induce arching action and net compressive forces in the beam. In a homogeneous elastic beam, in contrast, second order geometric effects lead to cable action with net tension forces. The arching action also leads to a reduction in the transverse stiffness, while the cable action has a stiffening effect.

4.2 ROLE OF COMPRESSIVE AXIAL FORCES

The model composed of discrete blocks can only be equilibrated by the presence of net axial compressive forces. In effect, the hangingwall beam acts as a shallow arch before closure takes place. The behaviour of arches has been described by Leontovich (1959), Timoshenko and Gere (1961), and Heyman (1971,1977). The compressive forces in the beam may arise from three independant mechanisms :

(i) "pre-existing" compressive forces

(ii) compressive forces induced by the dilation associated with shear slipping along the block interfaces in the beam itself

(iii) compressive forces induced by the arching action.

4.2.1 Pre-existing compressive forces

The compressive force due to the first mechanism cannot be easily quantified. Pre-existing compressive forces exist as a result of the horizontal virgin stress and slip along the shear fractures ahead of the stope face. The slip along the shear fractures results in horizontal dilation of the rock towards the mined out region.

University of Cape Town

4.2.2 Compressive forces due to shear slip

Shear slipping along the vertical fracture planes in the hangingwall beam itself results in dilation at the interfaces. This mechanism will be activated only to the extent that an increase in compressive force is necessary to maintain equilibrium. The significance of joint dilatancy associated with shear deformation is illustrated by a simplified analysis of the jointed beam in Figure 4.1. It must be emphasised that equilibrium is not satisfied in this analysis, but it does illustrate the magnitude of slip required at the joints to produce the axial compression to support the beam. Pender (1985) describes the dilatant behaviour of a beam with vertical joints.

A beam with a span of 100 m is considered in the analysis. The depth and width of the beam are 1 m. Shear deformation with associated dilatancy is permitted at the joints. The yield function is shown in Figure 4.2 with an associated flow rule for the dilatancy. The angle of friction ϕ along the interfaces is taken to be 20°. In this analysis, the blocks are not permitted to rotate. Assuming the beam to be initially supported along its full length, mining is simulated by removing the supports in steps, starting at the centre. It is assumed that all shear deformation takes place at the edge of the unsupported region where the maximum shear force occurs.

The axial force required to resist slip at the joint is given by

$$N = \frac{S}{\tan\phi}, \qquad (4.1)$$

where S is the shear force across the joint and ϕ is the angle of friction. The elastic axial deformation in the beam due to the axial force can be computed from Hooke's law and is given by

$$\delta = \frac{NL}{AE}, \qquad (4.2)$$

University of Cape Town

where L is the unsupported length, A the cross-sectional area and E is Young's modulus. The total shear deformation required to generate the dilatant axial displacement is given by

$$u = \frac{\delta}{\tan\phi} \quad . \qquad (4.3)$$

In this way the shear deformation required to generate an axial thrust to resist slip can be computed.

The shear displacements along the halfspan of the beam are plotted in Figure 4.3 for three different mining procedures. For case 1 the excavation is performed in a single step with all the shear deformation occurring at the support. The magnitude of the shear deformation is 7.28 mm and the axial force in the beam is 3 710 kN.

In case 2 the excavation is performed in steps of 1 m with deformations occurring during each step of mining. The midspan displacement resulting from shear locations of all the joints is 3.72 mm and the axial force in the beam is again 3 710 kN. For the case where the excavation is performed in steps of 1 m with external supports every 20 m, the shear deformations are that of case 3 in Figure 4.3.

The results show that relatively small displacements are required to support the system, indicating that the compressive forces due to dilatancy could contribute to the stability of the beam.

4.2.3 Compressive forces due to arching action

The compressive force due to arching action will also be activated only to the extent that an increase in compressive force is required to maintain equilibrium.

University of Cape Town

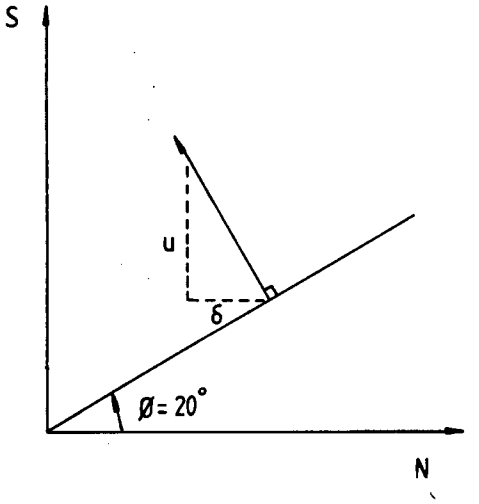

Figure 4.2 : Yield function

University of Cape Town

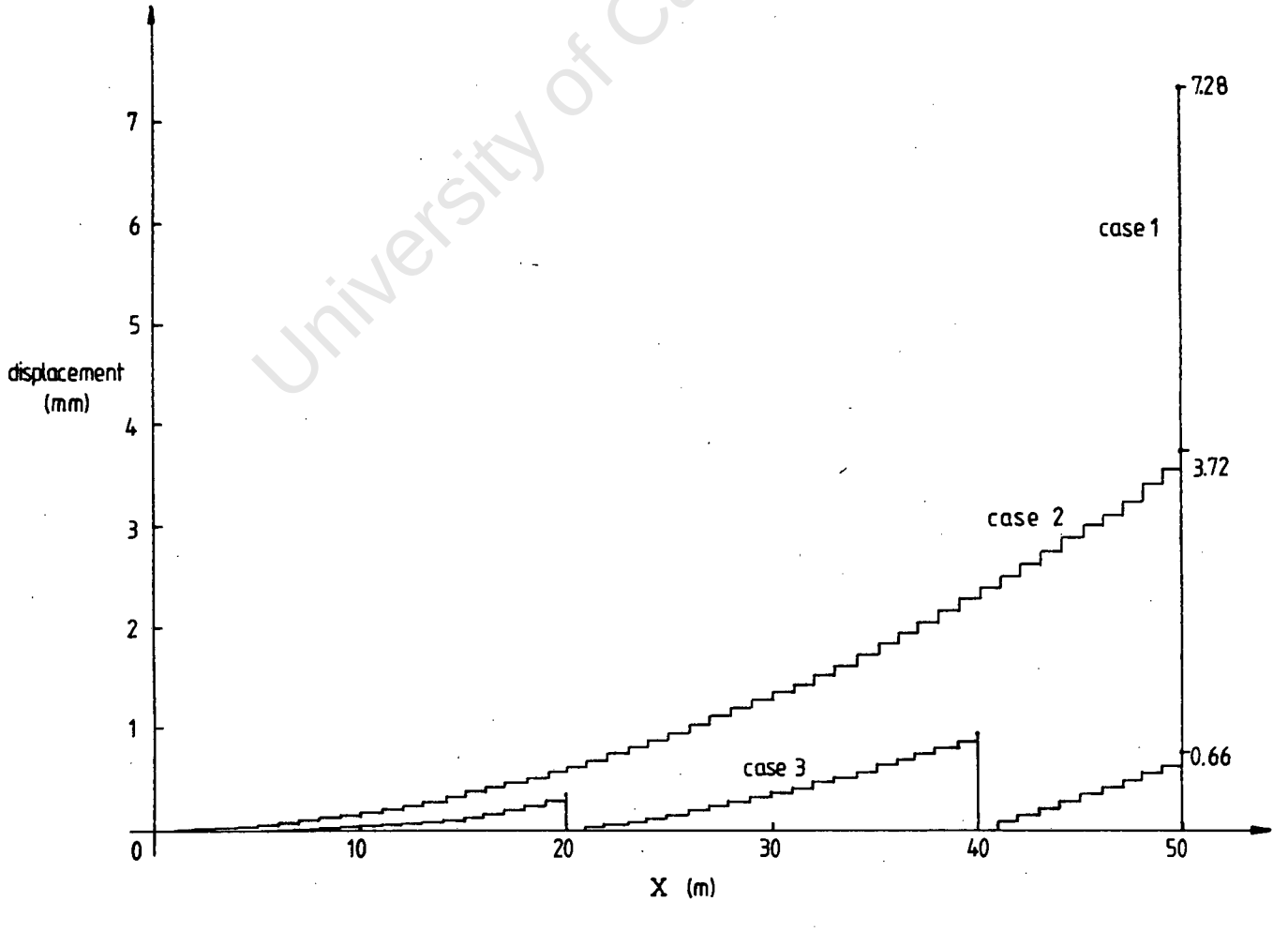

Figure 4.3 : Shear deformation of a beam with vertical fractures

4.3 LIMIT STATE APPROACH

We shall adopt a "limit state" approach and assume that there are no pre-existing compressive stresses. We shall further assume that no shear slip occurs across the interfaces in the beam and shall therefore concentrate only on the compressive forces due to arching action. These assumptions are justified by the observation that compressive forces due to the first two mechanisms will tend to increase the stability and reduce deflections of the beam; the assumptions are thus conservative.

The basic model we propose is shown in Figure 4.1. With this model we anticipate some of the important features of the behaviour of the hangingwall. There are three possible failure modes for this problem. Shear failure at the supports when the limiting shear resistance is less than the required vertical reaction; crushing at the hinges formed at the centre and at the supports; buckling of the beam to form an unstable, snap-through mechanism. We shall assume that the beam will not fail in either of the first two failure modes, and consider only the unstable, snap-through behaviour.

An important question is that of the largest unsupported span which can be stably equilibrated by the axial forces due to arching action alone. A further important question is the deflection of the beam at this point; will closure occur before the beam has a tendency to snap-through? Following on the answer to this question, we must then ask what additional requirements are necessary to permit "safe" closure i.e. to permit closure to occur without instability. Finally, we must ask whether the beam is stable after closure has occurred. These questions will be addressed in Chapter 5 by considering some simplifications of the basic model.

University of Cape Town

CHAPTER 5

BEHAVIOUR OF THE FRACTURED BEAM MODEL

5.1 INTRODUCTION

The model of the hangingwall beam proposed in Chapter 4 can be simplified by making assumptions about the number and position of active interfaces. By reducing the number of interfaces, we can make use of simple models to obtain qualitative answers to the questions raised about the behaviour of the mathematical model.

We will attempt to answer the various questions raised in section 4.3 by considering simplifications to the model of the beam shown in Figure 4.1. In these models it is relatively complex to follow the actual mining sequence where the gravity load is fixed and the span of the beam increases as the face advances. In this chapter we shall discuss models of a beam of fixed halfspan where the gravity load increases from zero to its full value. The object of these models is to gain insight into the essential features of the problem rather than to provide specific numerical results for particular cases.

The questions that will be addressed in this chapter are :

(i) What is the limiting unsupported span that can be stably equilibrated on the assumption of axial forces due to arching action alone?

(ii) What additional requirements are necessary to permit safe closure?

(iii) Is the beam stable after closure has occurred?

University of Cape Town

Three different models have been used to study the various aspects of the behaviour :

(i) Idealised block model

The basic model can be simplified by assuming that only three fractures are active, namely those at the supports and at the centre of the beam. This idealised model in which the beam is treated as two homogeneous blocks with hinge supports and a central hinge connection is used to determine the limiting unsupported span.

(ii) Truss model

The block model of (i) can be simplified to a truss model for which we can obtain an analytical solution. Concentrated load is applied to the centre of this model in order to identify the conditions for safe closure. The minimum support required for safe closure is determined using the same model with a distributed load and a single spring at the centre. The bending effects are later included to determine their effect on the behaviour.

(iii) Multiple interface model

A two-dimensional model of the hangingwall beam which includes a realistic representation of the vertical fracture planes is used to investigate the stability of the beam after closure has taken place.

5.2 LIMITING UNSUPPORTED SPAN

5.2.1 Idealised block model

We begin our study by considering the simple model shown in Figure 5.1. We treat the beam as two homogeneous blocks, with hinge supports at A and B and a hinge connection at C. This is highly idealised, assuming that only the interfaces at A, B and C are active, and that only point contact takes places at the interfaces. In this and subsequent models, we consider an

University of Cape Town

increasing gravity load for a fixed halfspan, rather than attempting to follow the actual behaviour where the gravity load is fixed and the span increases as the face advances.

The structure has been analysed using the plane strain finite element model shown in Figure 5.2, with nonlinear geometric effects included. In this analysis, Young's modulus and Poisson's ratio are taken to be 70 GPa and 0.2 respectively. The finite element code ABAQUS was used for this and all subsequent finite element analyses reported.

5.2.2 Discussion of results

Setting the selfweight equal to 27 kN/m^3, and the depth D = 1 m, Figures 5.3 and 5.4 show the horizontal reaction H and the central deflection as a function of the halfspan L. Two important conclusions can be drawn.

(i) The maximum halfspan which can support the selfweight of 27 kN/m^3 is slightly greater than 31 m. This in itself is an encouraging result, in the sense that it is in accord with what happens in practice; we must recognise that the simple model is stiffer than the model of Figure 4.1 since we have limited the number of active interfaces and we have overestimated the effective depth of the arch by placing hinges at A, B and C.

(ii) The deflection at the centre of the beam for the limiting halfspan is about 0.4 m, whereas closure would require a deflection of about 1 m. This indicates that closure will not occur for the limiting span for the selfweight of 27 kN/m^3.

The significance of this result is evident in Figure 5.5, where for a halfspan of 31 m we plot the load-central displacement relationship for an equilibrium solution. A Riks algorithm, which steps along the equilibrium path rather than the load path, is employed to obtain this solution. The

University of Cape Town

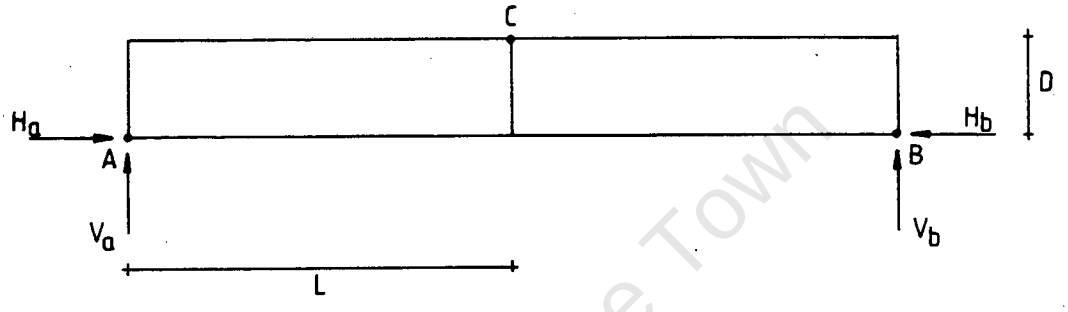

Figure 5.1 : Idealised block model of hangingwall beam

University of Cape Town

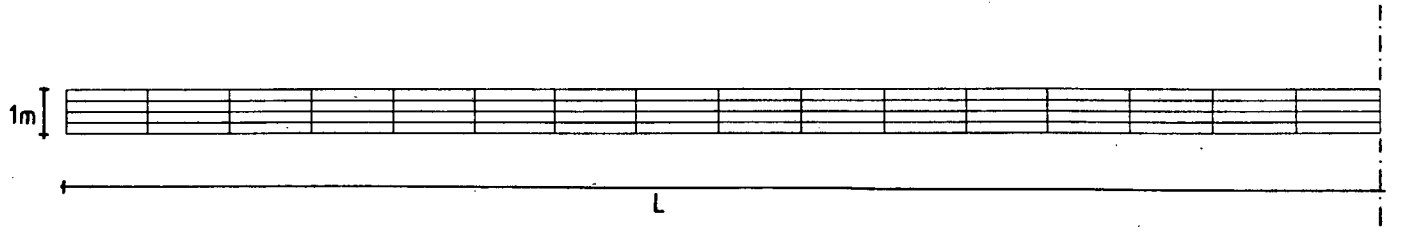

Figure 5.2 : Finite element mesh

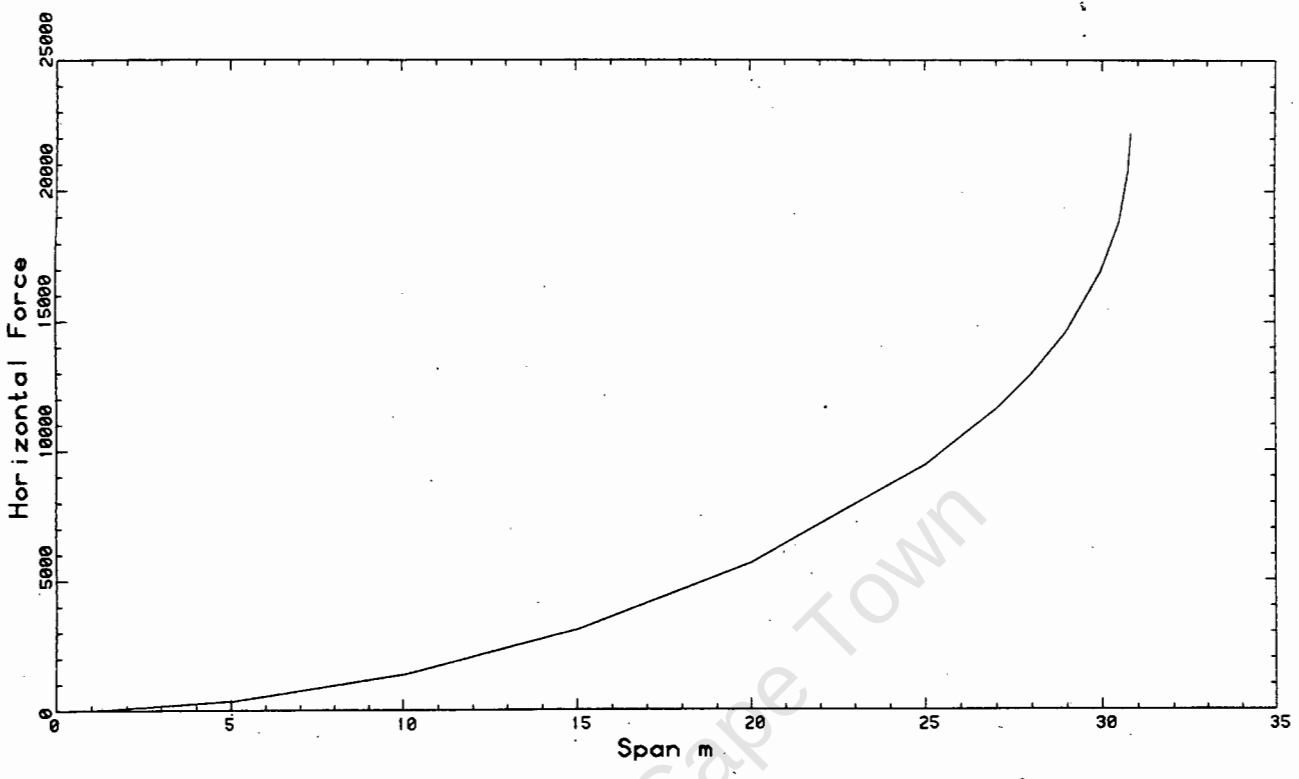

Figure 5.3 : Horizontal force vs halfspan

University of Cape Town

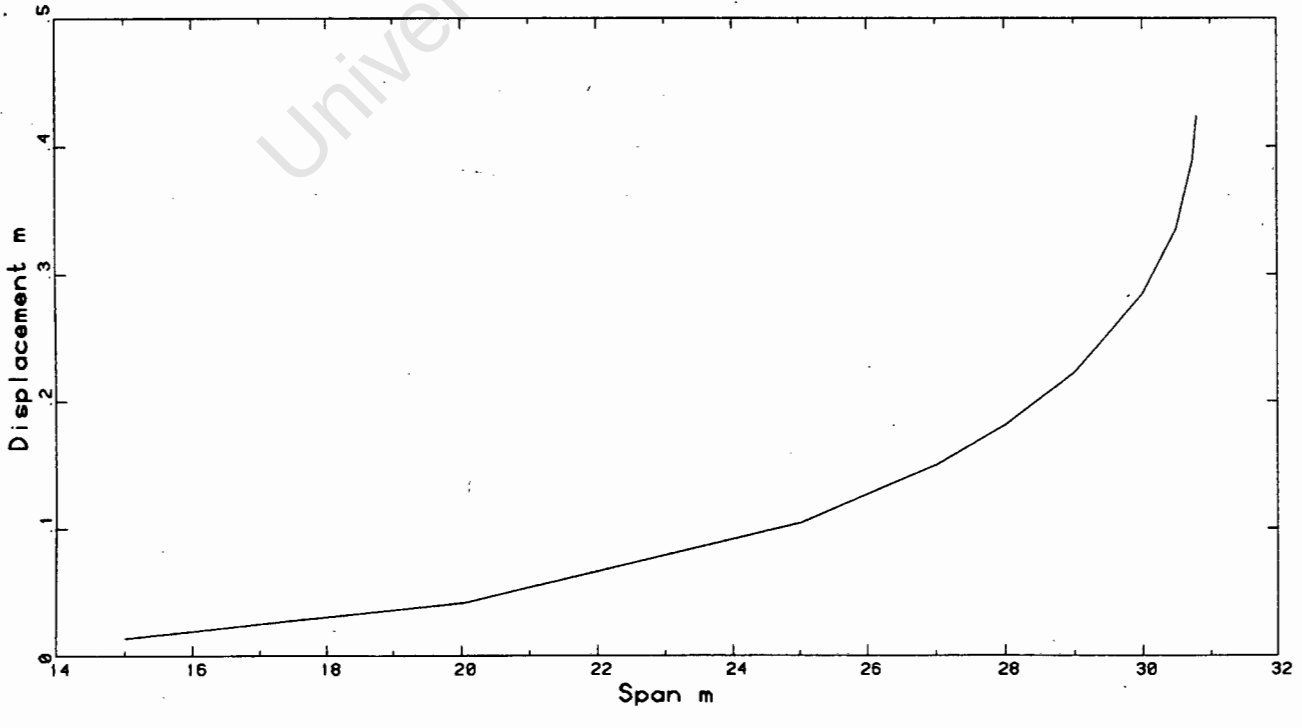

Figure 5.4 : Central deflection vs halfspan

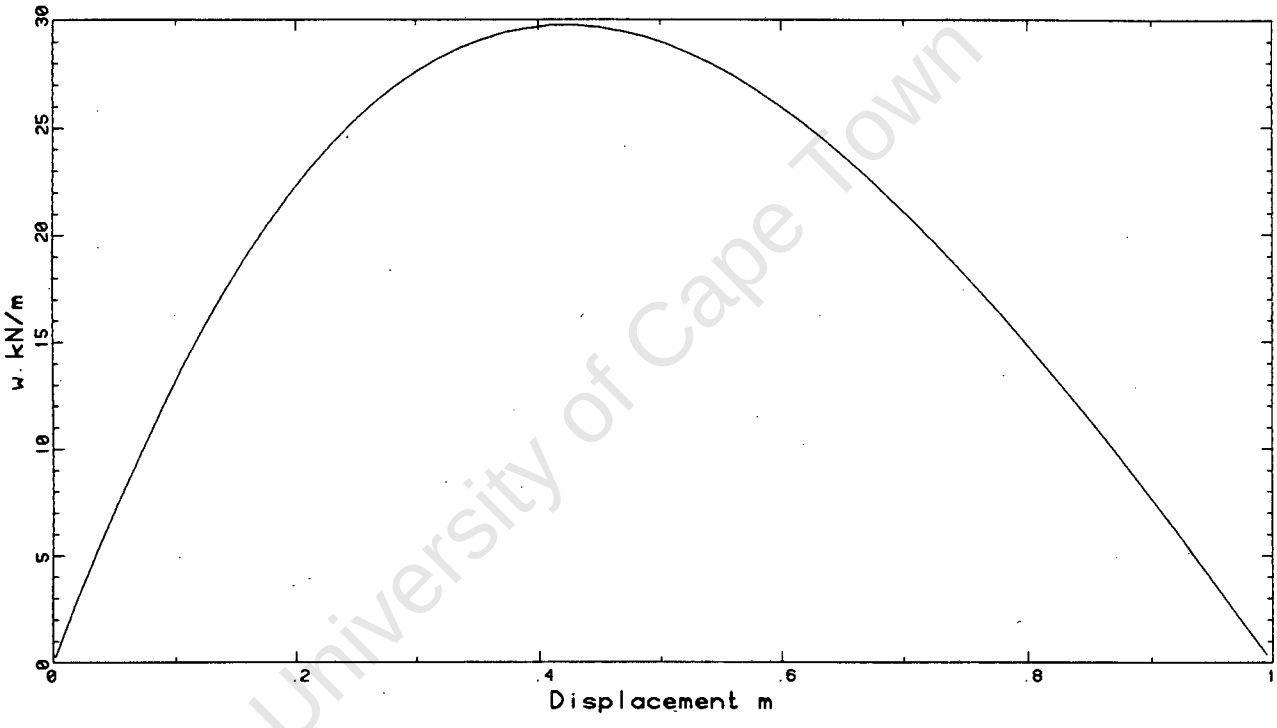

University of Cape Town

Figure 5.5 : Load-central displacement relationship

possibility of snap-through is clearly seen; the maximum load is reached at a deflection of 0.4 m, and the load must be decreased in order to maintain equilibrium as the deflection increases. In practice this means that if for a fixed gravity load of 27 kN/m³ the span were increased, an unstable failure of the beam would occur.

5.3 SAFE CLOSURE

The analysis of the model shown in Figure 5.1 shows that the maximum stable deflection of the beam is about 0.4 m, i.e. closure has not yet occurred. For stable closure to occur the deflection of the beam must be increased to 1.0 m (i.e. the assumed movement before closure takes place) when the full load is applied.

In order to investigate the conditions required to permit "safe" closure, a range of simplified models of the beam is studied. The first, a truss with a concentrated load, is used to identify the conditions for safe closure. The second, a truss with a distributed load, is used to quantify the results. Bending effects are included in a more realistic third model which is also subjected to a distributed load.

5.3.1 Conditions for safe closure

In order to determine the conditions required for safe closure, the very simple model in Figure 5.6 is instructive. Here we treat the structure as a truss, with no bending effects. The axial stiffness of the beam is retained and the load is treated as a concentrated load.

The model can be analysed in terms of Figure 5.7. For horizontal equilibrium

$$H_A = H_B \,. \qquad (5.1)$$

University of Cape Town

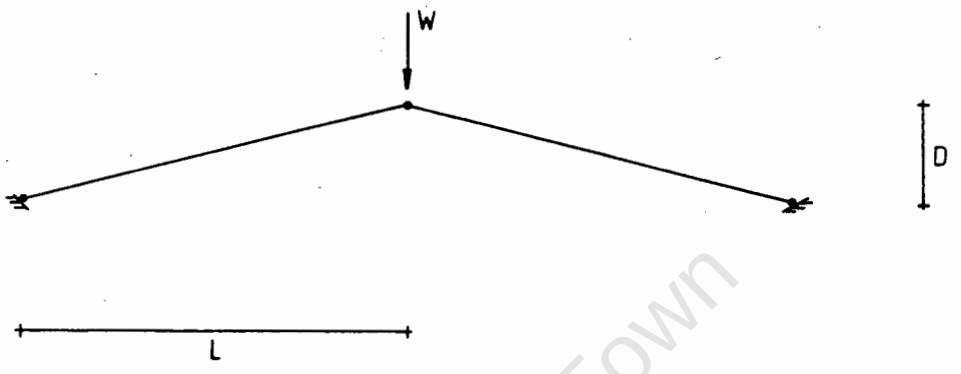

Figure 5.6 : Truss model with concentrated load

University of Cape Town

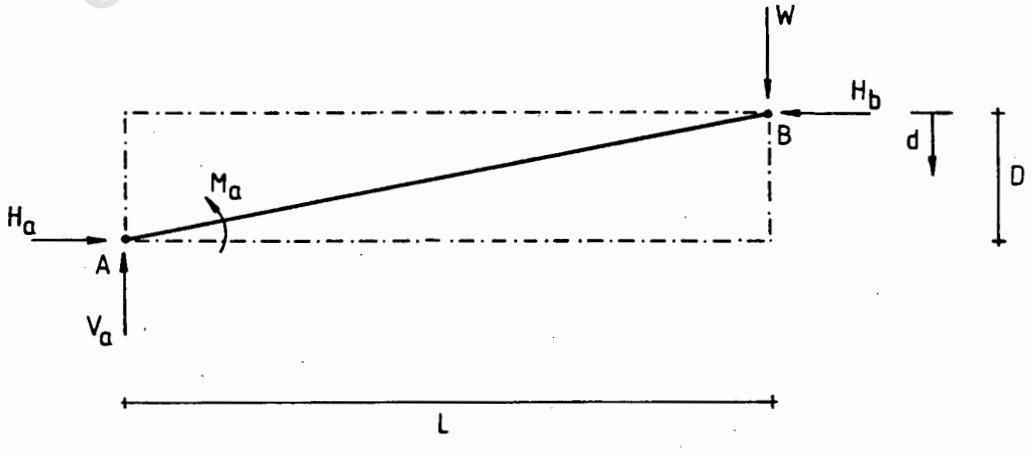

Figure 5.7 : Forces on the truss model

The sum of moments about point A yields the expression

$$-\frac{WL}{2} + H_B (D - d) = 0 \ , \qquad (5.2)$$

where

$$H_B = EA\epsilon \ . \qquad (5.3)$$

Assuming large strains,

$$\epsilon = \frac{2dD - d^2}{2 (L^2 + D^2)} \ . \qquad (5.4)$$

Substituting equations (5.3) and (5.4) into (5.2), yields the following expression:

$$-\frac{WL}{2} + EA \frac{2dD - d^2}{2 (L^2 + D^2)} (D - d) = 0 \ . \qquad (5.5)$$

Solving for W gives

$$W = \frac{EA}{L (L^2 + D^2)} (2dD - d^2) (D - d)$$

$$= \frac{EA}{L (L^2 + D^2)} (d^3 - 3Dd^2 + 2D^2d) \ . \qquad (5.6)$$

In order to obtain the maximum value of W, we can differentiate equation (5.6)

$$\frac{dW}{dd} = 0 \rightarrow 3d^2 - 6Dd + 2D^2 = 0 \ , \qquad (5.7)$$

therefore

$$d = 0.423 \ D \quad \text{or} \quad 1.577 \ D.$$

University of Cape Town

Now substituting $d = 0.423\ D$ into equation (5.6) yields

$$W_{max} = 0.385\ \frac{EAD^3}{L\ (L^2 + D^2)}\ . \qquad (5.8)$$

The concentrated load W is expressed in terms of the central deflection d in equation (5.6). We find that instability occurs at about the same displacement as in the previous analysis, namely at about 0.4 m. This result is encouraging as it shows the similarity between the behaviour of the idealised block model and the truss model.

In order to permit safe closure, we need to increase the deflection before instability occurs. Certain parameters are varied to note the effect on the maximum deflection.

(i) Depth

By increasing the depth D of the beam, the peak load increases and the deflection at peak load increases linearly. Figure 5.8 shows the effect of changing D on the load-displacement curve. The deflection at a fixed load is reduced with an increase in depth.

(ii) Span

Varying the span affects the peak load reached; the peak load is larger for smaller spans. The deflection at which the peak load is reached is not changed by varying the span. This is shown in Figure 5.9.

(iii) Compressive force

Pre-existing compressive forces are present in the hangingwall beam. The effect of applying an initial horizontal force of H_o to the structure is shown in Figure 5.10. The beam is stiffer but snap-through initiates at a smaller displacement.

University of Cape Town

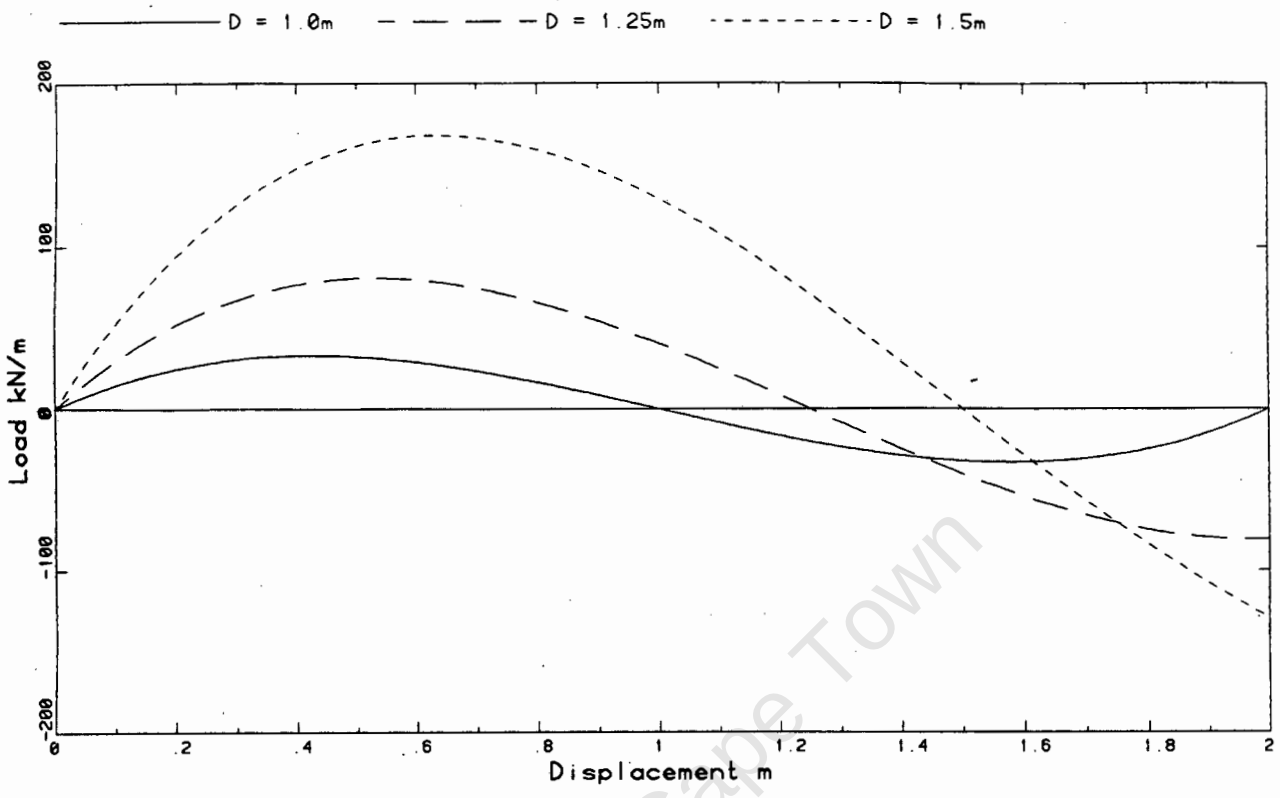

Figure 5.8 : Effect of varying depth D

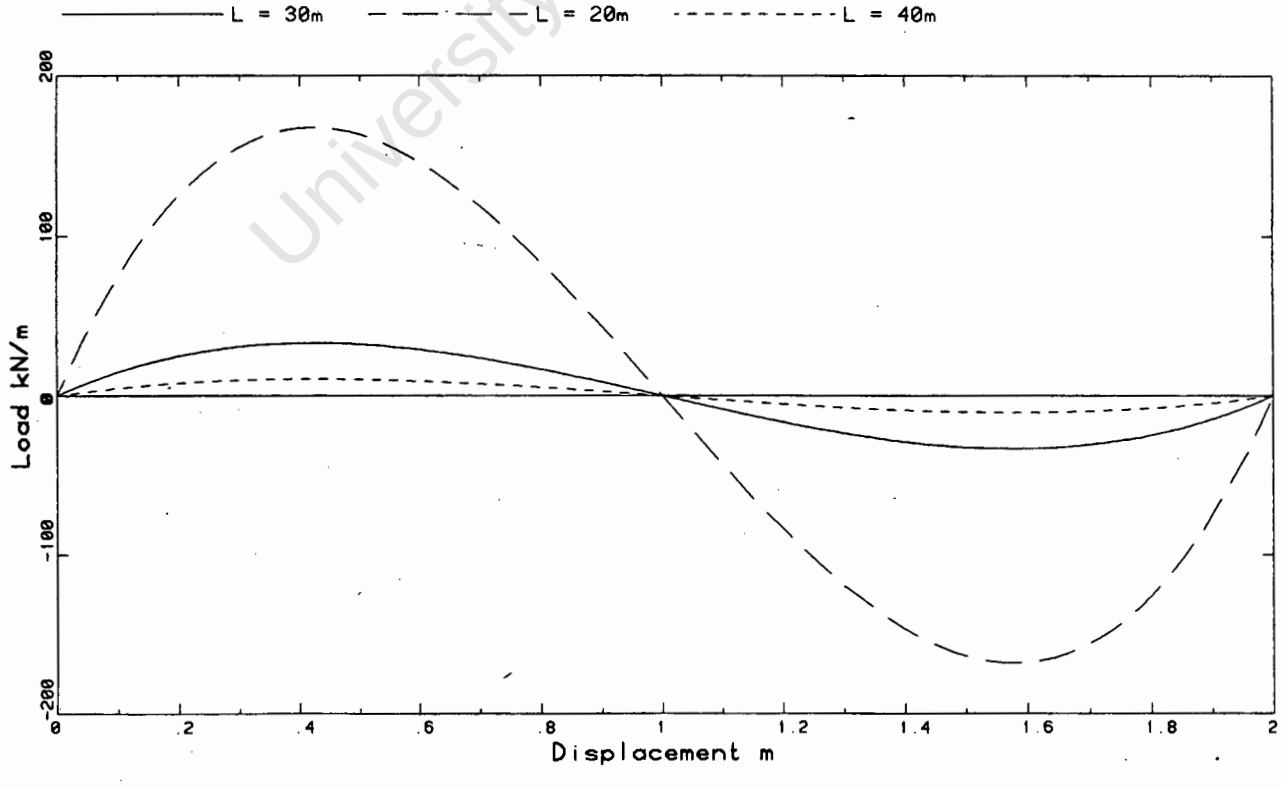

Figure 5.9 : Effect of varying halfspan L

University of Cape Town

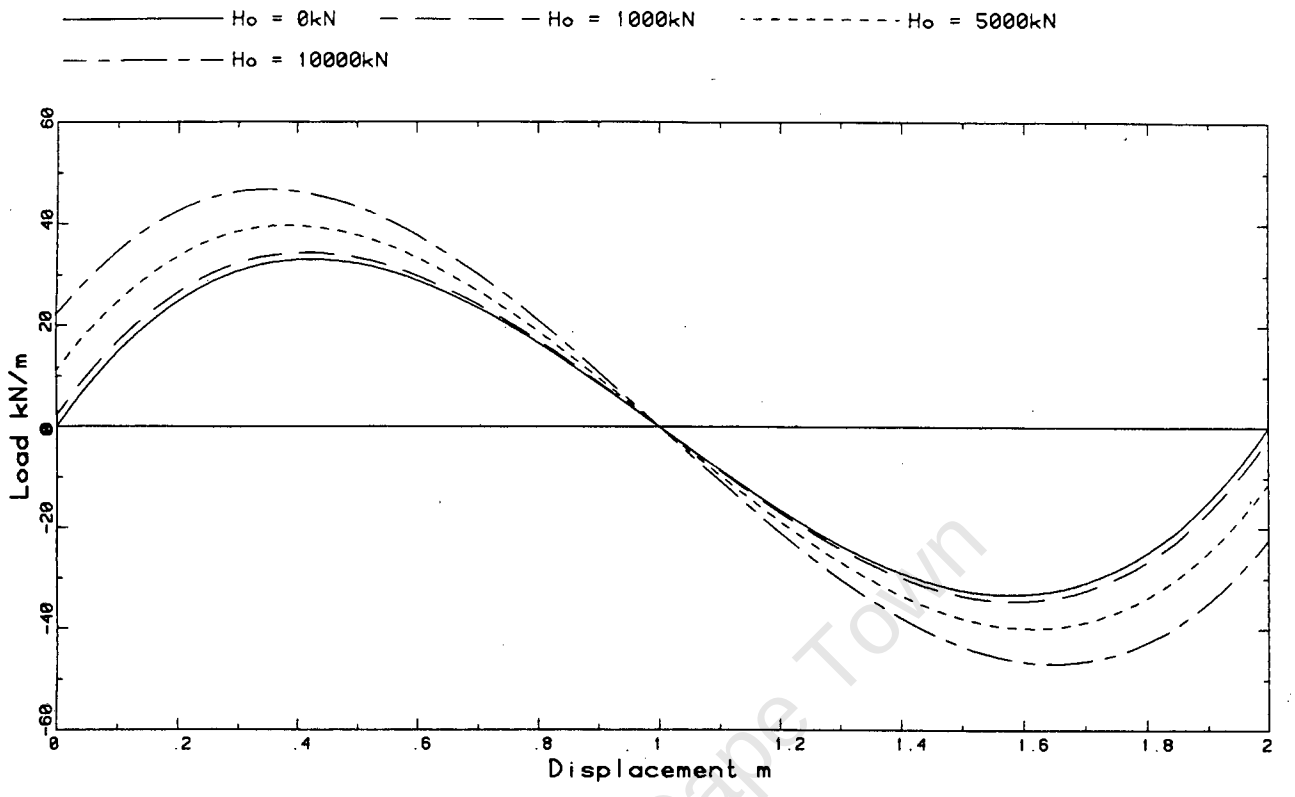

Figure 5.10 : Effect of varying initial compression H_o

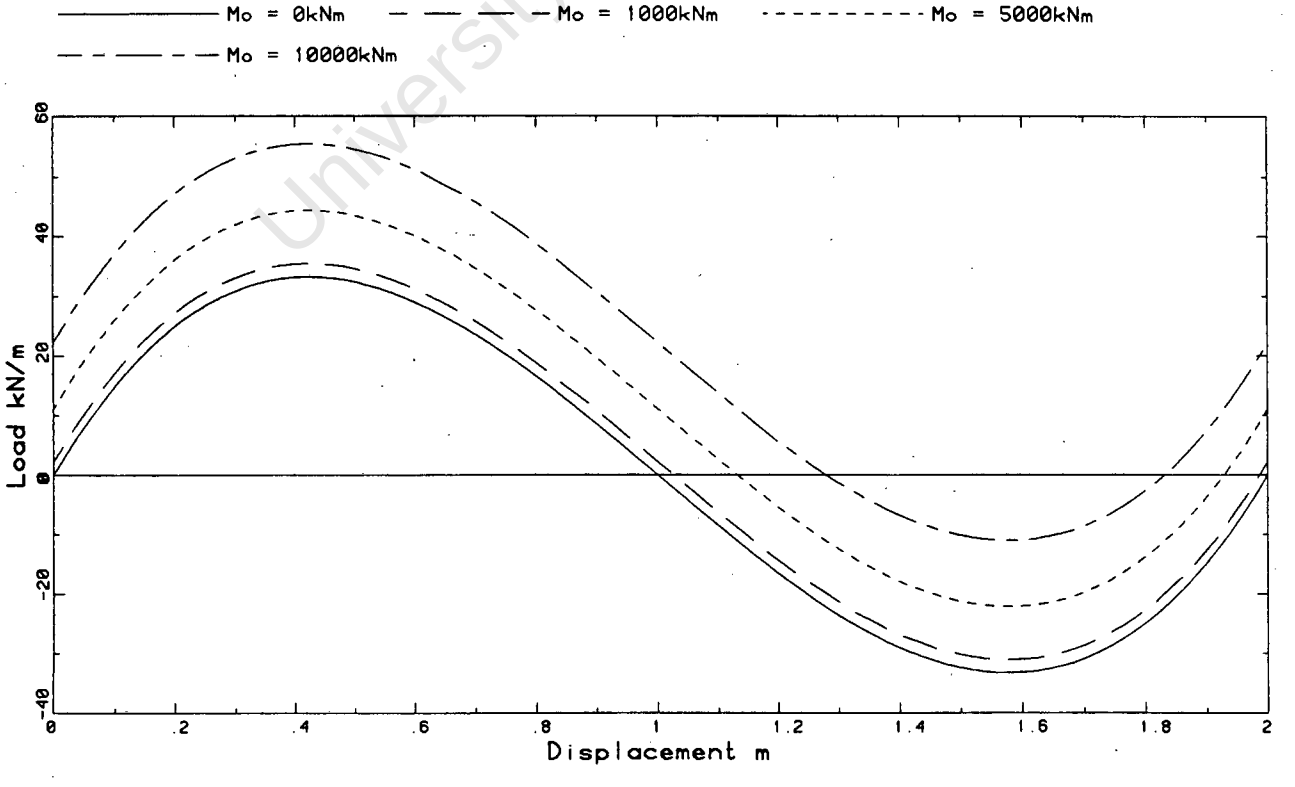

Figure 5.11 : Effect of varying applied moment M_o

University of Cape Town

(iv) Applied moment

This model assumes pinned connections at the supports. In order to include rotational stiffness a moment M_o can be applied at the support. The effect of applying an end moment M_o to the structure is shown in Figure 5.11. The graph is displaced vertically by changing the applied moment, but the displacement at the peak load does not change.

It is clear from the preceeding discussion that safe closure will not be achieved by changing any of the above variables. In order to achieve safe closure the structure needs to be supported in the central region and "let down" until closure has taken place. The support can be provided in this model by a single spring at the centre as shown in Figure 5.12.

The limiting load-displacement relationship for stable closure is represented by the relationship OAC in Figure 5.13. This implies that the force-displacement relationship for the supporting spring must have the form represented by the shaded area in Figure 5.13. Such a spring will "let down" the hangingwall beam safely onto the footwall, without a snap-through failure.

The force-displacement relationship for the supporting spring can be calculated by

$$F(d) = W_{max} - W(d) \quad . \tag{5.9}$$

Substituting equations (5.8) and (5.6) into (5.9) gives

$$F(d) = 0.385 \frac{EAD^3}{L\,(L^2 + D^2)} - \frac{EA}{L\,(L^2 + D^2)}\,(d^3 - 2Dd^2 + 2D^2d) \tag{5.10}$$

$$= \frac{EA}{L\,(L^2 + D^2)}\,(0.385\,D^3 - d^3 + 2Dd^2 - 2D^2d) \quad .$$

University of Cape Town

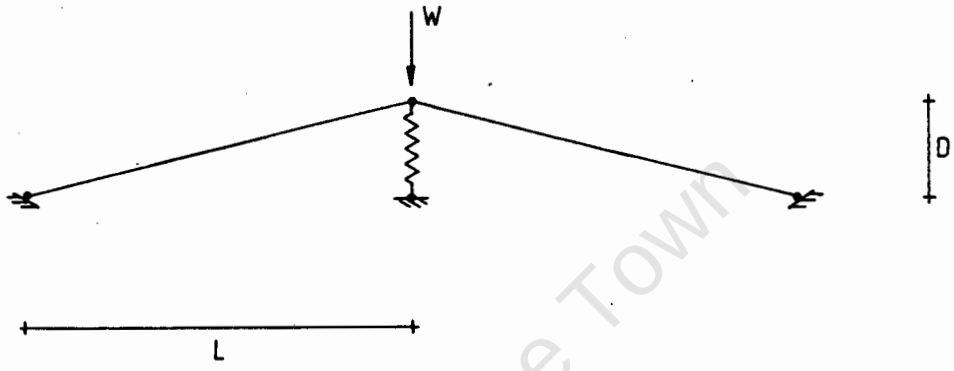

Figure 5.12 : Truss model with central supporting spring

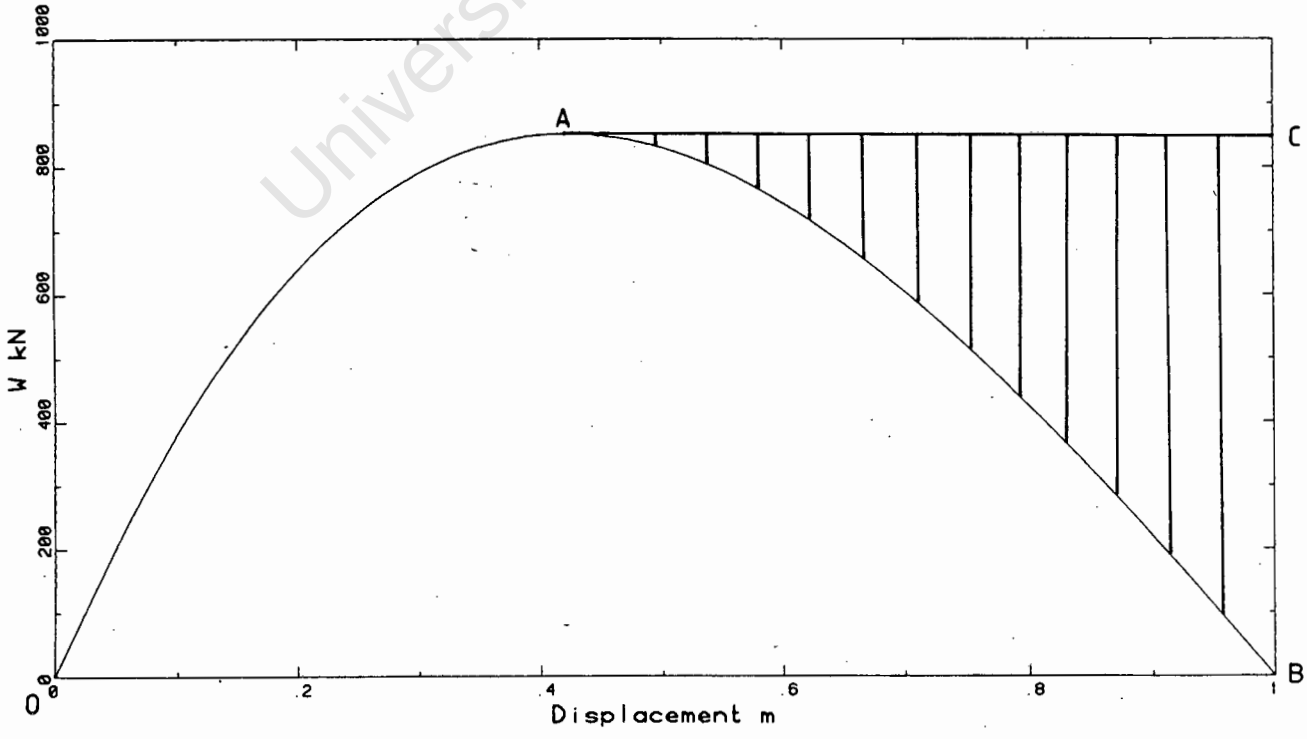

Figure 5.13 : Load-displacement relationship

University of Cape Town

5.3.2 Minimum support for safe closure

The analysis of the model shown in Figure 5.6 shows that some additional support is necessary to allow closure to occur safely. While the support can, in practice, be provided in a variety of ways, this study is limited to considering the minimum support required at the centre of the beam.

The model used to determine the minimum support required is the same truss used above, but in this instance carrying a uniformly distributed load w as shown in Figure 5.14. Support is provided in the centre by a single spring.

The model can be analysed in terms of the parameters described in Figure 5.15. The sum of moments about point A yields the expression

$$- \frac{wL^2}{2} + H_B (D - d) + FL = 0 \ . \qquad (5.11)$$

This differs from equation (5.2) in that the $\frac{WL}{2}$ term is now $\frac{wL^2}{2}$.

Following the same assumptions as before, the load w can be expressed as

$$w = \frac{EA}{L^2 (L^2 + D^2)} (d^3 - 2Dd^2 + 2D^2d) + \frac{2F}{L} \ . \qquad (5.12)$$

Maximising equation (5.12) we find that

$$w_{max} = 0.385 \frac{EAD^3}{L^2 (L^2 + D^2)} + \frac{2F}{L} \qquad (5.13)$$

when

$$d = 0.423 \ D \quad \text{or} \quad 1.577 \ D \ .$$

University of Cape Town

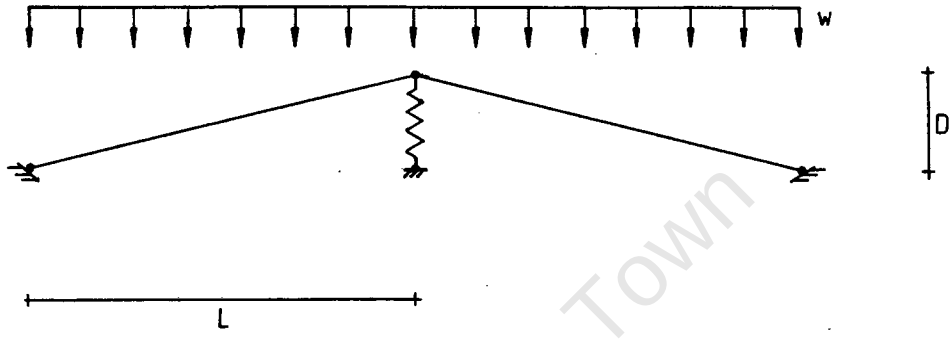

Figure 5.14 : Truss model with distributed load

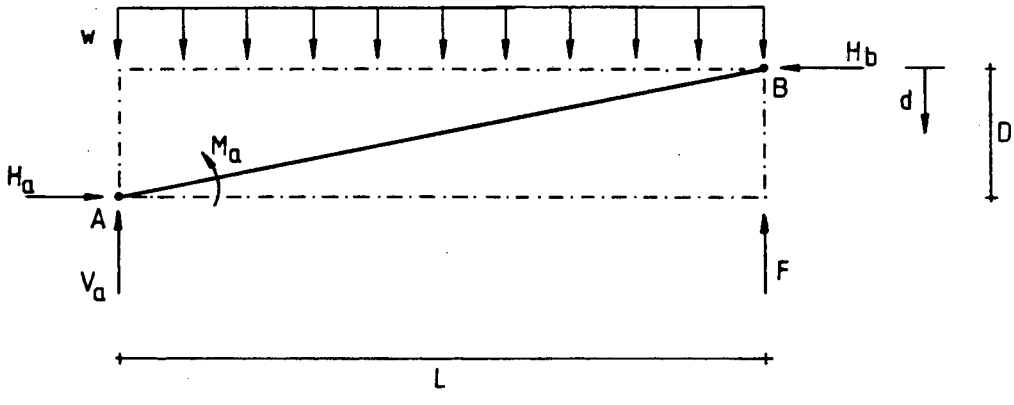

Figure 5.15 : Forces on the truss model

University of Cape Town

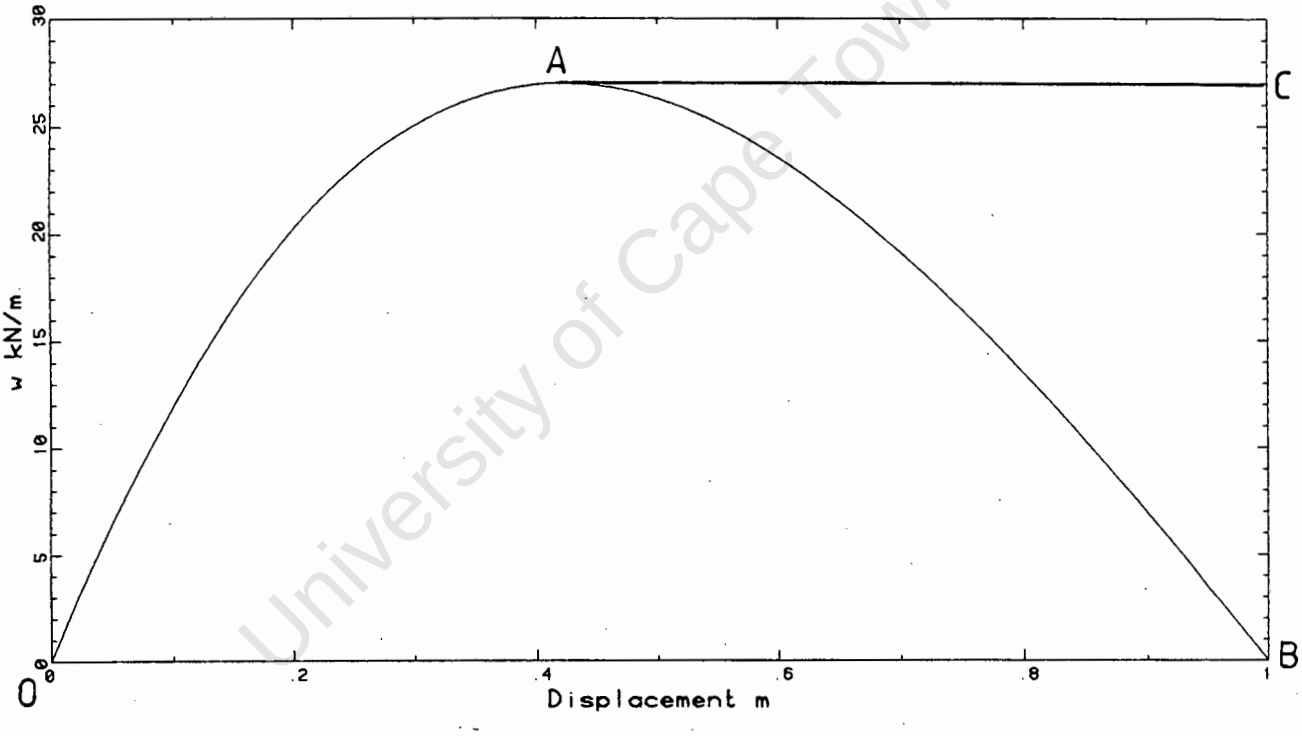

University of Cape Town

Figure 5.16 : Load-displacement relationship for truss model

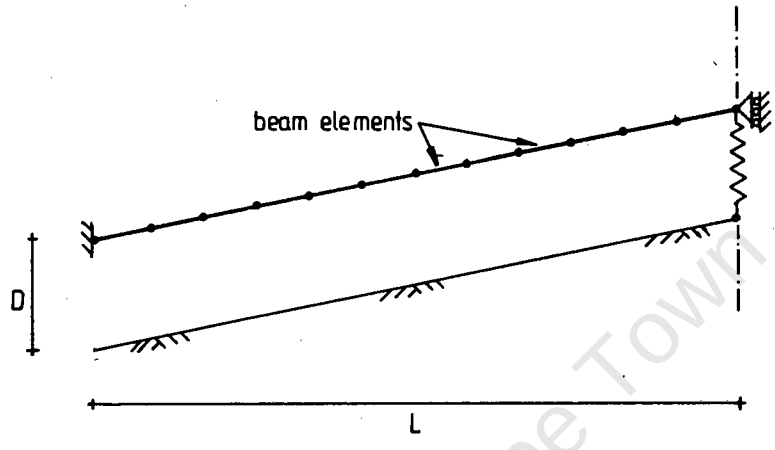

Figure 5.17 : Beam model for hangingwall beam

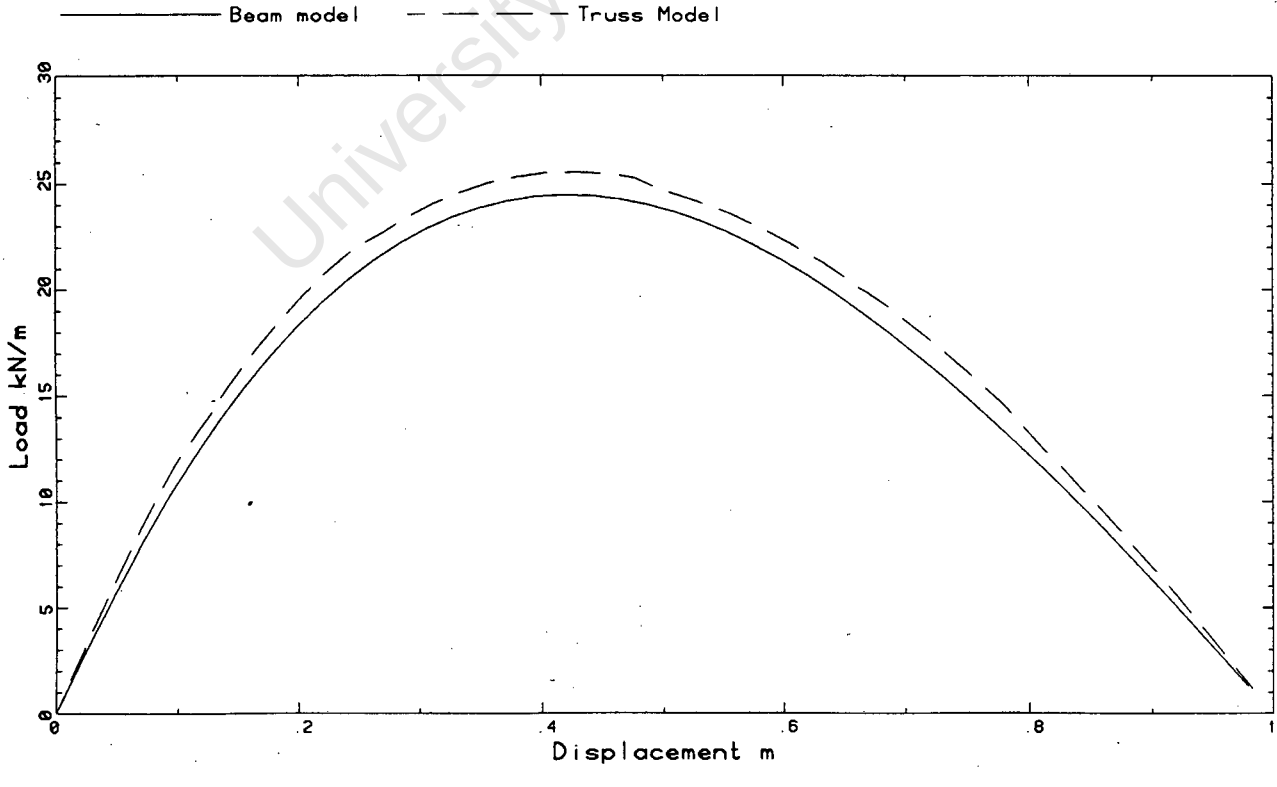

Figure 5.18 : Load-displacement relationship for beam model compared to that of the truss model

University of Cape Town

shown by the dashed curve. It is seen that the maximum value is lower when beam elements are used. This is due to the inclusion of deflections caused by bending, making the model less stiff.

A central support spring with a characteristic given by equation (5.15) is required for the limiting case of safe closure. This characteristic curve is shown in Figure 5.19. With such a support the load-displacement relation of Figure 5.18 remains near horizontal after the peak load until the hangingwall meets the footwall. This is shown in Figure 5.20.

5.4 STABILITY OF THE BEAM AFTER CLOSURE

The simple analyses given in the previous section indicate that additional external support is essential to "let down" the hangingwall beam to effect safe closure. The nature of the external support, in the limiting case, is seen in Figure 5.19. We now ask whether the hangingwall is stable after closure has taken place. This is a fundamental question, since the position after closure is representative of the steady state in which the face and the point of closure advance together. In addressing this point, we will introduce a two-dimensional planar model of the hangingwall beam which also includes a realistic representation of the vertical fracture planes. This model represents very closely the basic model depicted in Figure 4.1.

University of Cape Town

5.4.1 Description of the planar model

Once again a beam of fixed span will be considered in this analysis. The vertical fracture planes in the hangingwall beam are modelled by means of interface elements. Separation between adjacent blocks is permitted across these interface elements, but tangential slip is prevented by applying a multiple point constraint (MPC) on each fracture plane. These MPC's are placed on the edge of the fracture planes where compressive stresses are anticipated. In the cases where tensile stresses are present, adjacent blocks must be free to separate. It is expected that the separation of blocks will be localised in the areas where the bending moments are the largest. For this reason it is necessary

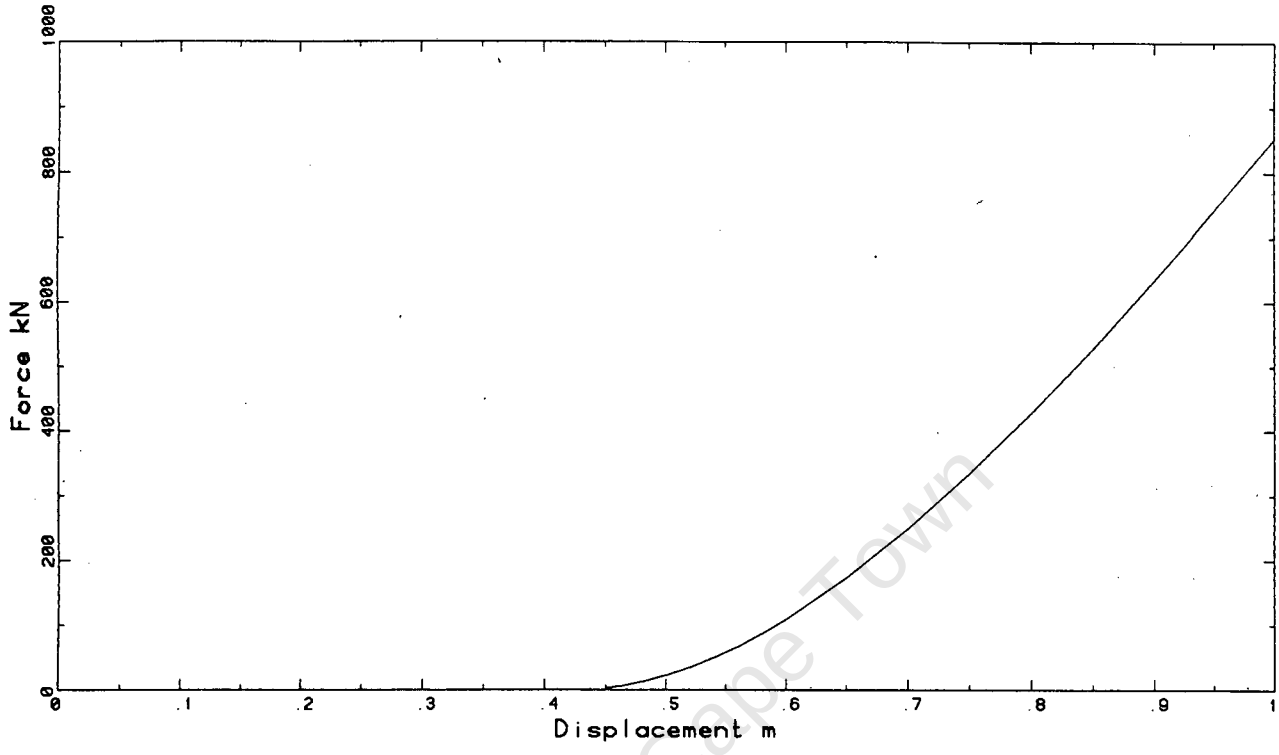

Figure 5.19 : Force-displacement relationship for the spring

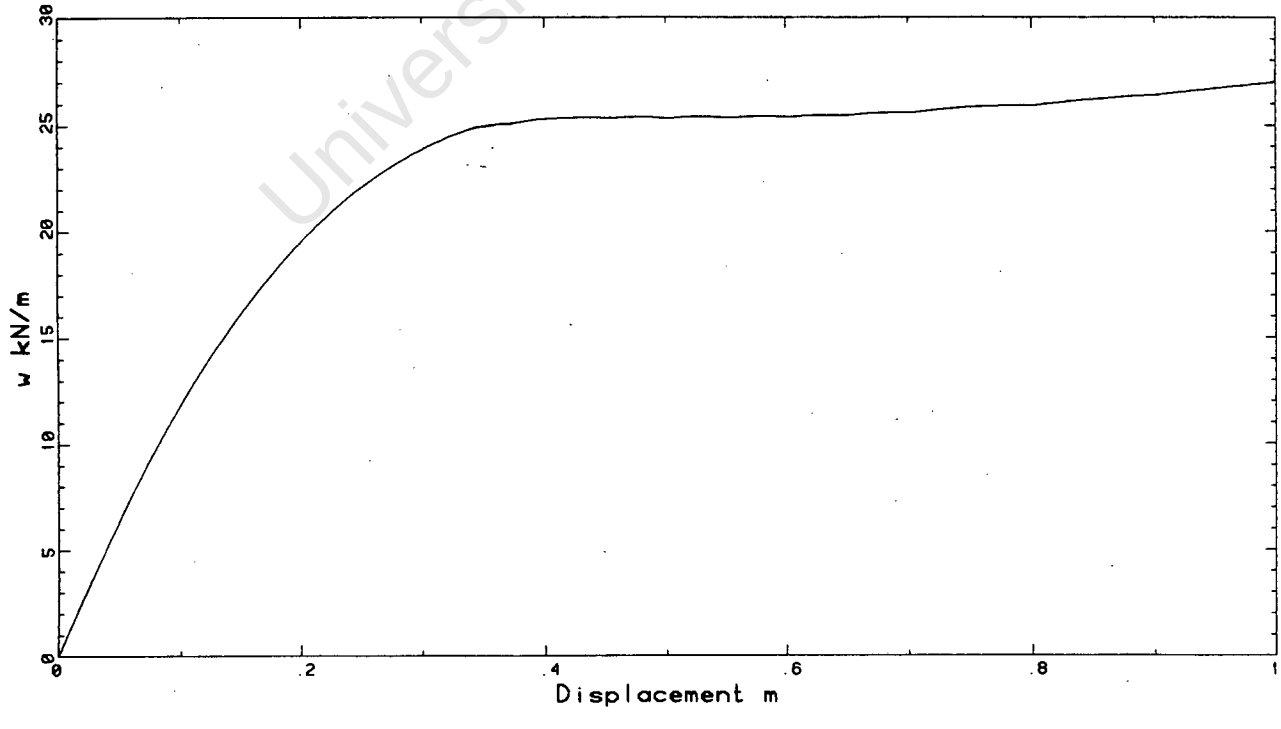

Figure 5.20 : Load-displacement relationship for the beam model with a central supporting spring

University of Cape Town

to include interface elements only at and near the support and around the centre. An initial analysis was done with a single interface at the support and at the centre. This simple model shows that separation occurs on the tension side of the interfaces at the support as well as in the centre.

The more realistic model of Figure 5.21 has a number of interfaces at the support and at the centre of the beam. We anticipate that this model will be less stiff than one with single interfaces at the support and at the centre.

The beam is modelled with two-dimensional plane strain elements. The rock is modelled using eight-noded serendipity elements with a Young's modulus and a Poisson's ratio of 70 GPa and 0.2 respectively. The fracture planes are modelled using six-noded interface elements with a friction coefficient of 0.2.

The finite element mesh is finely graded near the supports and at the centre where separation of the blocks takes place. Large elements are used in the zone where bending moments are smaller and separation is not expected to occur. Gap elements are used to constrain the displacement of the beam to a maximum of 1 m, in order to model the closure of the stope.

In these models a central supporting spring is not included, but the equilibrium path is followed until closure occurs at the central node. The load is then again increased and the deflections of the nodes on the soffit are monitored. Because the model does not permit irreversible inelastic strain, the state of the beam when the full load is reached for the second time will be no different from what it would have been if the beam had been let down in a stable manner. The results we obtain will thus be a realistic picture of the situation of the beam after closure has occurred.

University of Cape Town

5.4.2 Discussion of results

The results obtained confirmed that the multiple interface model is less stiff than the model which has single interfaces at the support and at the centre. The load-displacement relationship for the beam is shown in Figure 5.22. The load factor on the vertical axis is a factor applied to a reference load of 27 kN/m^3 (the selfweight of the rock). The peak load once again occurs at a displacement of about 0.4 m as was the case in the previous analyses. The load factor reaches its peak well below unity as this model is less stiff than previous models.

In order to assess the stability of the beam after closure, the analysis follows the equilibrium path of Figure 5.22 until closure occurs at the central node. The corresponding load is zero. The load is once again increased and the load-displacement relationship for a number of nodes on the soffit of the beam are shown for this extended analysis in Figure 5.23.

The displaced shape of the beam for a load factor of unity is shown in Figure 5.24. Closure has occurred only at the central node. Figures 5.25 (a) and 5.25 (b) show in greater detail the interfaces at the supports and at the centre of the beam. The points marked with an "x" are the Gauss points on the interface elements where separation has not occurred. These figures illustrate the extent of the zone in which separation occurs. The separation is more evenly distributed in the centre of the beam where the moment gradient is smaller. There is still a large amount of separation at the interface furthest from the centre indicating that separation would extend further from the centre if more interfaces were present.

Figure 5.23 shows us that the load-displacement curve has a positive slope for all points along the beam when the load factor is unity. It can thus be inferred that the equilibrium state for a unit load factor is stable.

University of Cape Town

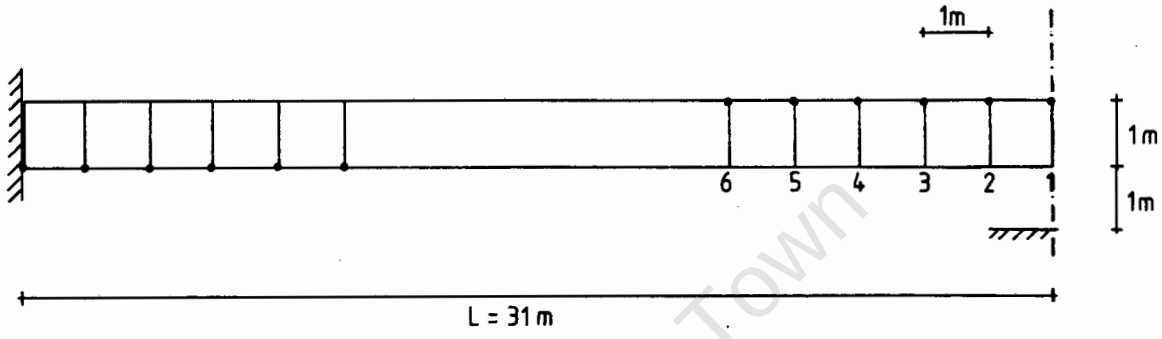

Figure 5.21 : Multiple interface model

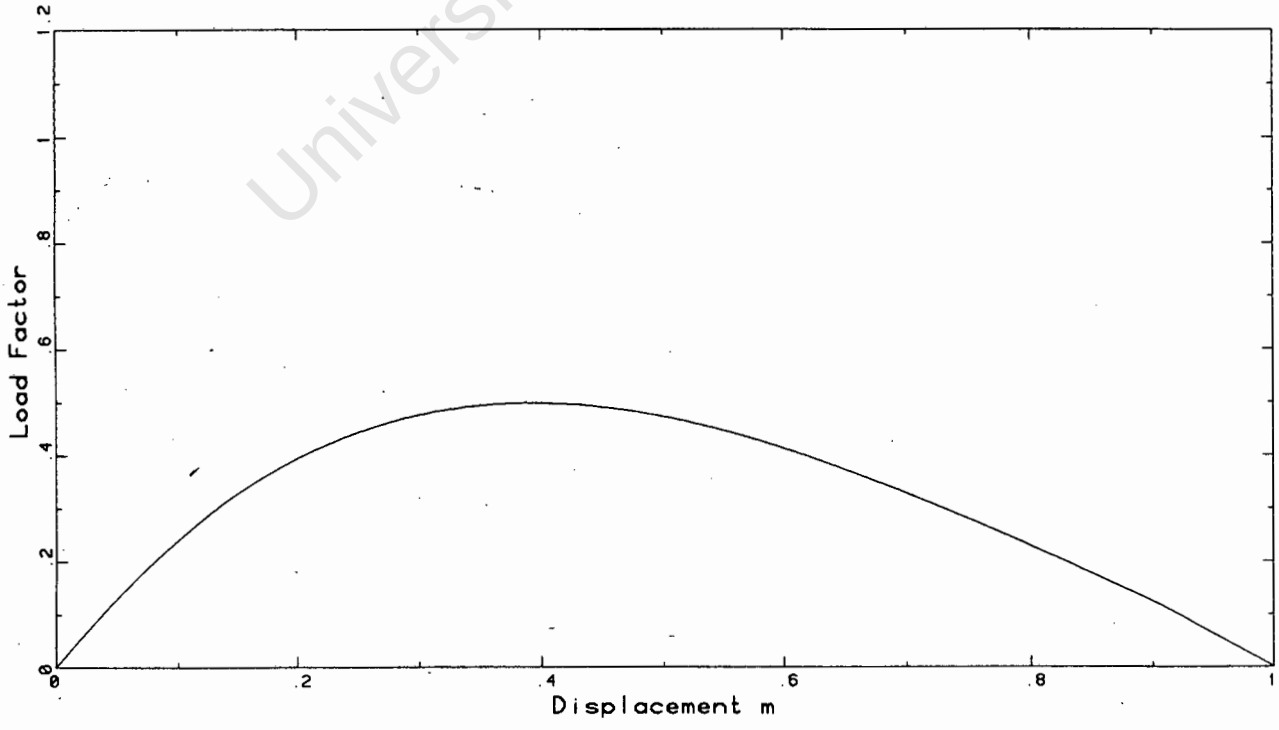

Figure 5.22 : Load-displacement relationship

University of Cape Town

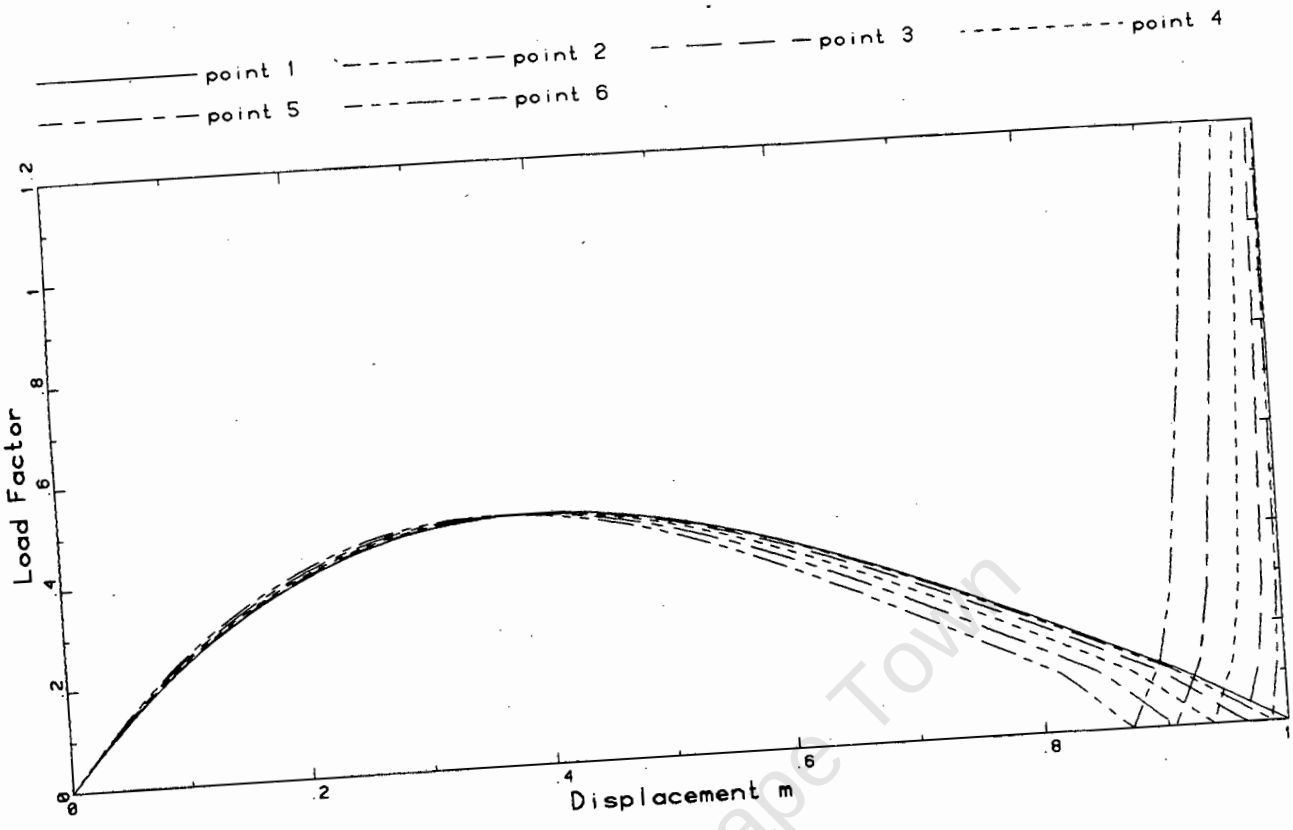

Figure 5.23 : Load-displacement relationships for nodes along the soffit of the beam

University of Cape Town

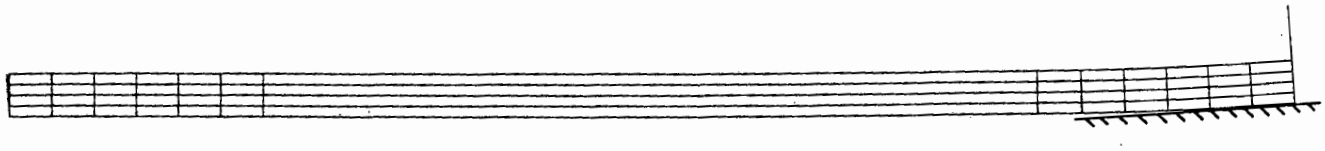

Figure 5.24 : Displaced shape at full load

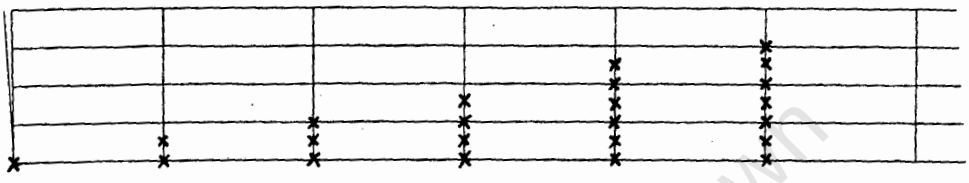

(a) Support detail

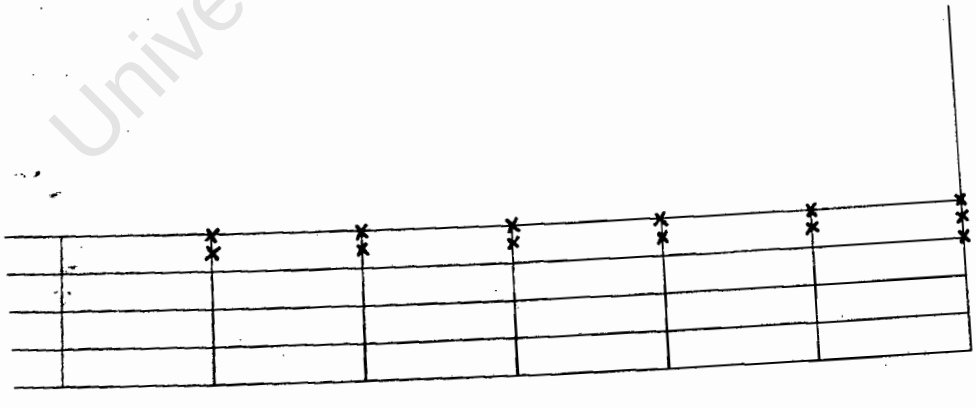

(b) Centre detail

Figure 5.25 : Separation along the interfaces

University of Cape Town

CHAPTER 6

SEQUENTIAL MINING MODEL

6.1 INTRODUCTION

The analyses presented thus far have used models where the span of the stope is fixed, and the weight of the hangingwall beam is gradually increased from zero to its full load. These models have given insight into the essential features of the problem and have answered a number of questions that were raised about the behaviour of the hangingwall beam. The beam exhibits unstable "snap-through" behaviour if the span is increased beyond a certain point. The halfspan at which "snap-through" takes place is about 30 m, but it depends on the model used. We have shown that stable closure of the stope takes place if sufficient support is provided and that the beam is stable once closure has occurred.

Following on from these findings it is of interest to investigate the behaviour of a realistically loaded stope in which the face advances as mining progresses. In practice the point of closure of the excavation advances as the face advances, suggesting a "steady state" in which the hangingwall beam has a configuration of the form shown in Figure 6.1. The stope remains the same, but moves as the face advances. A number of questions regarding the "steady state" configuration can be addressed by considering a finite element model of a stope with an advancing face.

A useful feature of ABAQUS is the model change option. This feature allows elements to be removed from an existing model in a load step. The sequential mining operation can thus be modelled by removing existing elements from beneath the hangingwall to simulate the advancing stope face. We shall use such a model to determine the features of the steady state configuration. Specific points that will be addressed are the distance between the point of closure and the advancing face, and the axial compression in the hangingwall beam.

University of Cape Town

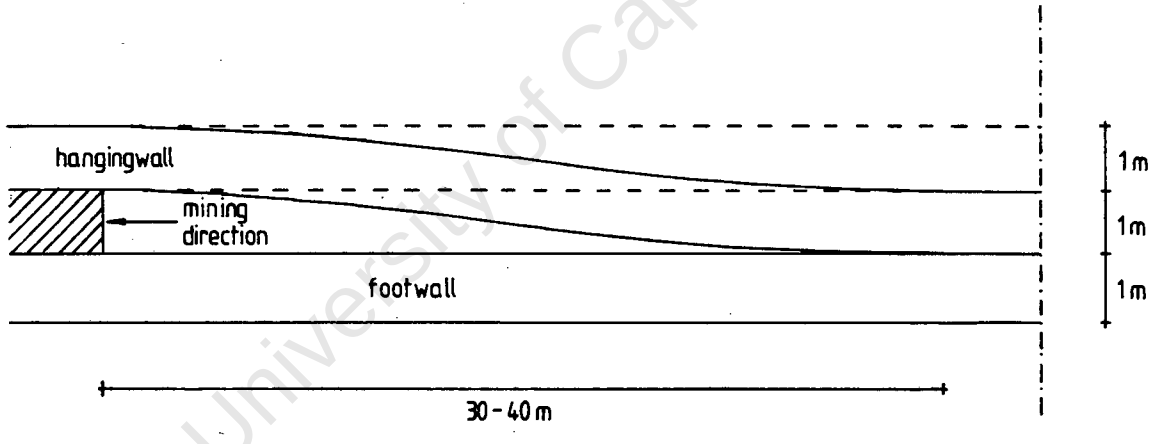

University of Cape Town

Figure 6.1 : Steady state configuration

6.2 DESCRIPTION OF THE MODEL

The hangingwall beam is modelled using the finite element mesh in Figure 6.2. A two-dimensional plane strain model is used. The beam is 1 m deep and has vertical joints at 1 m spacing. The intact blocks of rock are modelled with eight-noded serendipity elements having a Young's modulus of 70 GPa and a Poisson's ratio of 0.2. The joints are modelled with six-noded interface elements. Separation across the interface elements between adjacent blocks is permitted, but tangential slip is prevented. Two-noded gap elements are used on the soffit of the beam to limit the deflection to the closure distance of 1 m.

The purpose of this model is to simulate the process of sequential mining of the stope. The length of excavated stope therefore increases as the mining progresses. An initial analysis was performed to determine the limiting unsupported span for this model. Figure 6.3 shows that the limiting halfspan is about 27 m. This is in accord with what is expected; this model will be less stiff than the model composed of two homogeneous blocks which has a limiting unsupported span of 31 m. No solution is obtained for spans beyond 27 m, so it will be used as a starting point for the analysis after a Riks algorithm has let down the beam at the centre.

The support provided by the unmined rock is modelled using very stiff elastic spring elements. Horizontal and vertical springs are used to provide stiffness in both directions. Figure 6.4 shows the positioning of the spring elements on each homogeneous block. A 50 m length of hangingwall beam will be considered, 23 m of which is initially supported by horizontal and vertical springs and 27 m of which is unsupported.

The selfweight of the beam is applied and a Riks algorithm is used to "let down" the hangingwall beam to effect closure. In this model we do not include a central supporting spring, but follow the equilibrium path

University of Cape Town

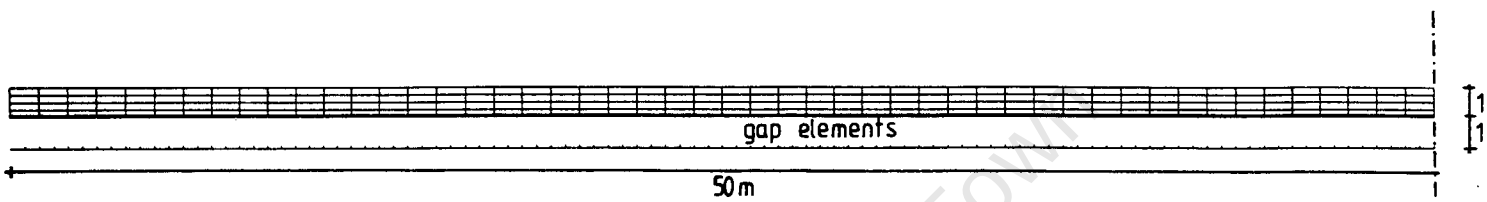

Figure 6.2 : Finite element mesh for advancing face model

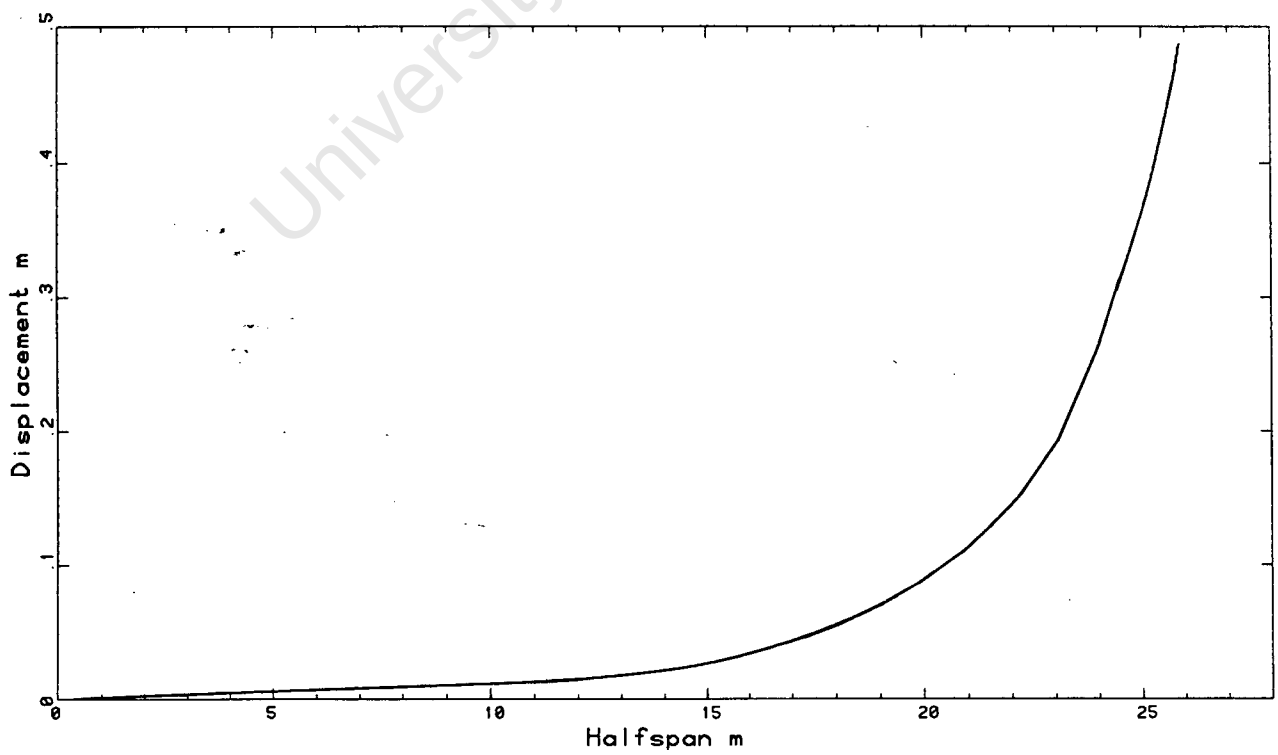

Figure 6.3 : Deflection vs halfspan for sequential mining model

University of Cape Town

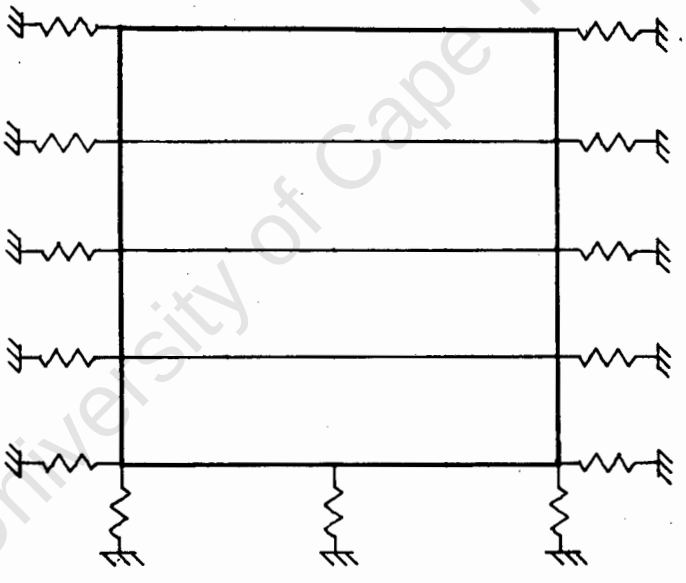

University of Cape Town

Figure 6.4 : Location of supporting springs on a typical block

until closure occurs at the central node and then increase the load again. Once a stable state is reached after closure, the springs are removed in steps of 1 m to simulate the advancing stope face.

The displaced shape of the hangingwall beam at progressive stages in the analysis are shown in Figure 6.5. In order to determine at what point a steady state configuration is attained, we need to look at the displaced shapes to find out when the shape is identical to that of the previous mining step. To do this we shall take the vertical displacement of the soffit of the beam as being representative of the overall displaced shape. The vertical displacement of the soffit of the beam from the stope face back to the mined area is plotted in Figure 6.6 at progressive stages in the analysis. It can be seen on Figure 6.6 that the curves become superimposed when the length of unsupported beam is approximately 34 m. This means that a steady state in the displaced shape has been reached. The configuration of the hangingwall beam remains the same, but advances with the stope face as the unsupported span increases beyond 34 m.

6.3 STEADY STATE CONFIGURATION

We shall now study the steady state configuration of the hangingwall beam to determine the essential characteristics. Aspects that will be studied are the shape, the zones where separation takes place, and the forces in the beam.

The displaced shape of the hangingwall beam which is representative of the steady state is shown in Figure 6.7. The distance from the stope face to the point of closure is 34 m. Figure 6.8 is a schematic representation showing the interfaces which have separated and the axial force in the beam. The separation is confined to a fairly small region at the stope face but is more evenly spread around the point of closure. The entire depth is in compression at the centre of the halfspan and in the region where closure has already occurred. The compressive stress is uniformly distributed through the depth of the beam in the latter

University of Cape Town

region and has a magnitude of 13 MPa. This model does not assume friction between the contacting hangingwall and footwall so the stress of 13 MPa implies that there is an axial compressive force of 13 000 kN in the beam.

This model, which simulates the progressive mining of the stope, has provided some insight into the steady state configuration of the hangingwall beam.

University of Cape Town

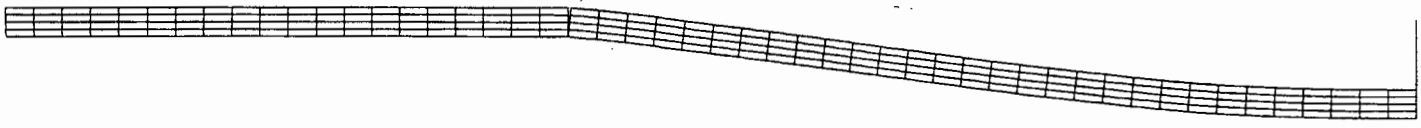

(a) 30 m unsupported

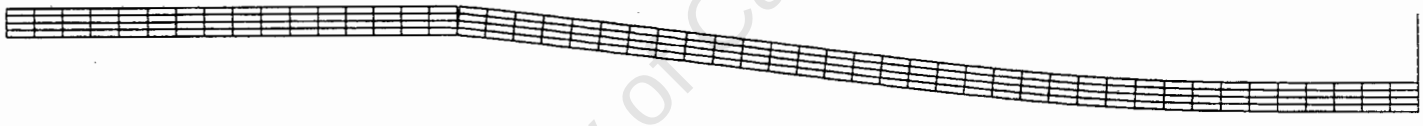

(b) 34 m unsupported

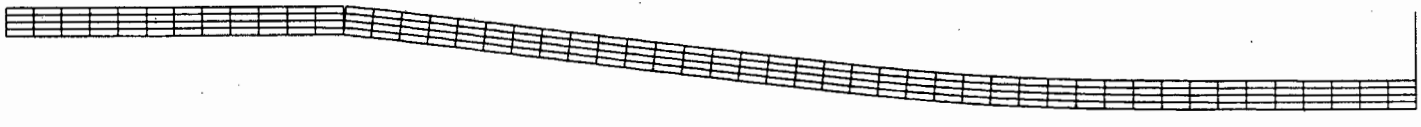

(c) 38 m unsupported

Figure 6.5 : Displaced shape at progressive stages in the analysis

University of Cape Town

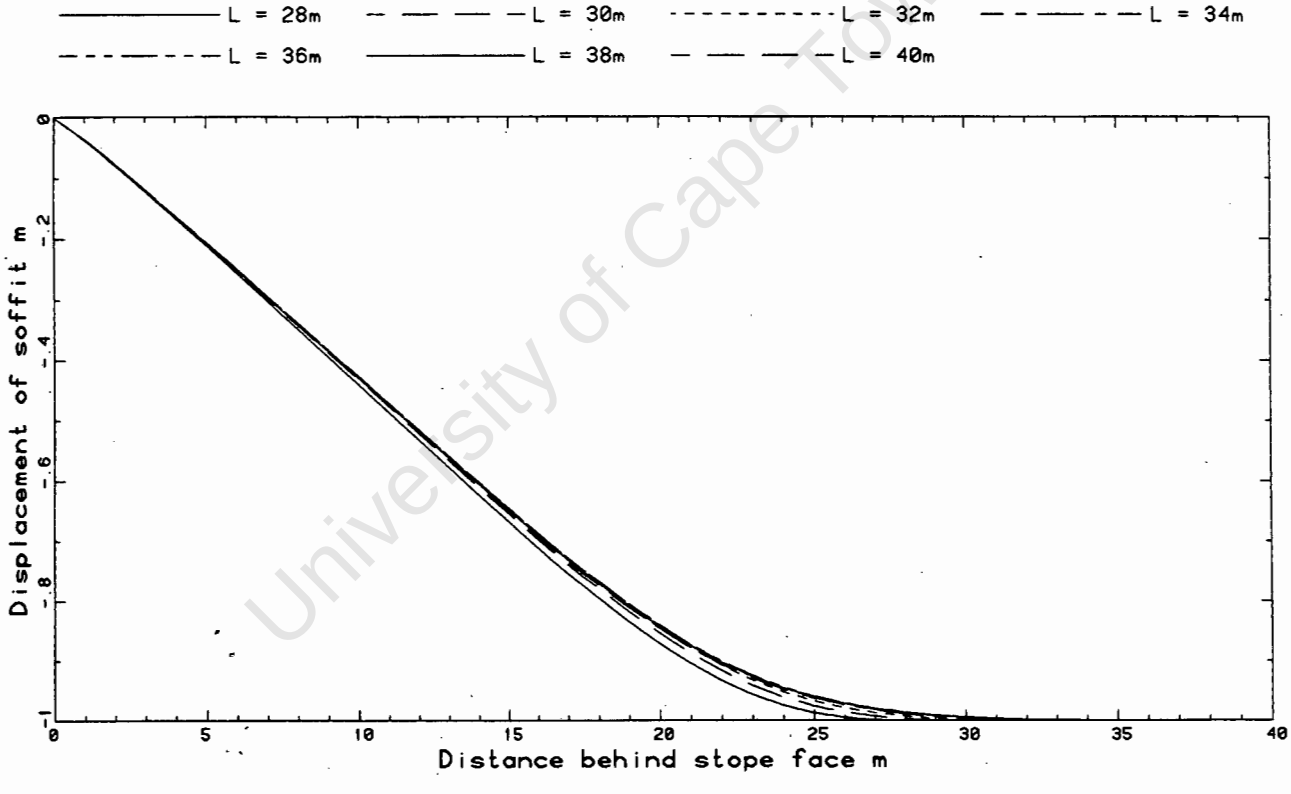

University of Cape Town

Figure 6.6 : Displacement of soffit at progressive stages in the analysis

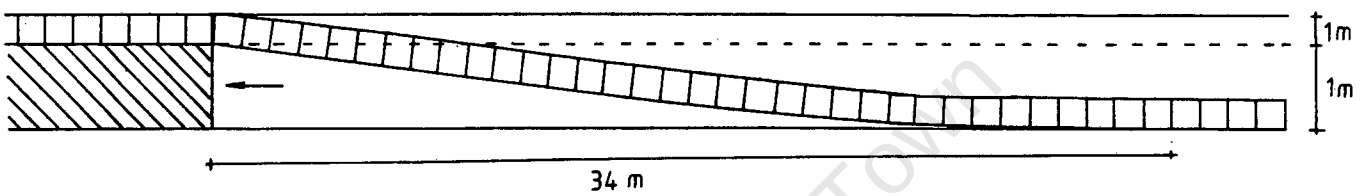

Figure 6.7 : Steady state configuration
The displacement is not to scale

University of Cape Town

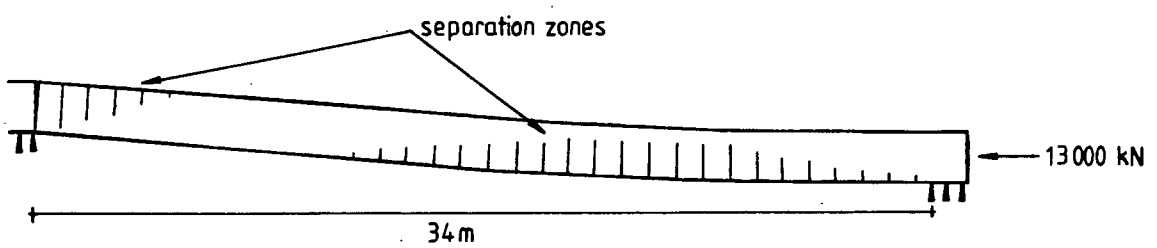

Figure 6.8 : Separation zones and forces in the steady state configuration

CHAPTER 7

CONCLUSIONS

The analyses which have been presented in this thesis are limited to simple models of the hangingwall beam. In spite of their simplicity, several broad conclusions regarding the behaviour can be drawn from the models. These are as follows:

1. Support is essential to permit first closure of the stope without snap through buckling. This can be achieved in a variety of ways, but it seems that a stiffening spring characteristic is optimal. Further study is needed to investigate how effective various actual support systems are.

2. Once closure has occurred, the hangingwall beam is stable in the global sense without additional support and without induced horizontal forces. The existence of supports and horizontal forces due to dilation will tend to increase the stability and stiffness of the hangingwall beam.

Recommendations for further work are as follows:

1. A study of the effectiveness of actual support systems used in the mines should be carried out.

2. The horizontal forces in the beam, particularly the pre-existing forces and those due to dilation at the shear fractures, need to be quantified more accurately and their effect on stability of the hangingwall beam should be studied.

3. The models presented are concerned only with global stability. Local effects, particularly those resulting from adversely inclined failure planes, clearly need further study. It is anticipated that support is essential to ensure local stability.

University of Cape Town

4. The stability of the hangingwall beam will be affected by dynamic disturbances. It is thus recommended that further work be carried out to study the stability of the hangingwall beam under dynamic loads.

5. The models used in this study have assumed the blocks of which the hangingwall is made up to be homogeneous and elastic. The stresses at contact points can be high resulting in local crushing at the hinges. It is suggested that further work include non-linear behaviour in the rock, especially at the hinges.

6. The assumption of plane strain, which permits the hangingwall to be treated as a beam, should be examined critically. In reality, the hangingwall will behave as a plate, and the out-of-plane bending will have some influence on the behaviour.

University of Cape Town

REFERENCES

ADAMS, G R, JAGER, A J and ROERIG, C (1981) "Investigations of Rock Fracture Around Deep Level Gold Mine Stopes", Proceedings 22nd US Symposium on Rock Mechanics, MIT, Cambridge MA.

BATHE, K-J (1982) Finite Element Procedures in Engineering Analysis, Prentice-Hall Inc, New Jersey.

BEER, G (1985) "An Isoparametric Joint/Interface Element for Finite Element Analysis", Int J Num Meth Eng, 21, 585-600.

BRADY, B H G, and BROWN, E T (1985) Rock Mechanics for Underground Mining, George Allen and Unwin.

BRUMMER, R K (1985) "A Simplified Modelling Strategy for Describing Rockmass Behaviour Around Stopes in Deep Hard-rock Gold Mines", in Research & Engineering Applications in Rock Masses (ed E Ashworth), Balkema, 113-120.

BRUMMER, R K and CROOK, A J L (1985) "The Development and Application of Finite Element Techniques for Modelling the Inelastic Behaviour around Mining Excavations", Proceedings of the Symposium on Finite Element Methods in South Africa, Stellenbosch, 110-130.

BRUMMER, R K (1987) "Fracturing and Deformation at the Edges of Tabular Gold Mining Excavations", PhD Thesis, Randse Afrikaanse Universiteit.

COOK, R D (1974) Concepts and Applications of Finite Element Analysis, Wiley and Sons.

DESAI, C S, ZAMAN, M M, LIGHTNER, J G and SIRIWARDANE, H J (1984) "Thin-layer Element for Interfaces and Joints", Int J Num & Anal Meth in Geomech, 8, 19-43.

EVANS, W H (1941) "The Strength of Undermined Strata", Trans Inst Min Metall, 50, 475-532.

University of Cape Town

GHABOUSSI, J, WILSON, E L and ISENBERG, J (1973) "Finite Element for Rock Joints and Interfaces" J Soil Mech and Foundation Div, ASCE, 99, SM10, 833-848.

GOODMAN, R E, TAYLOR, R L and BREKKE, T L (1968) "A Model for the Mechanics of Jointed Rock", J Soil Mech and Foundations Div, ASCE, 94, SM3, 637-659.

GOODMAN, R E and DUBOIS, J (1972) "Duplication of Dilatency in Analysis of Jointed Rocks", J Soil Mech and Foundation Div, ASCE, 98, SM4, 399-422.

GOODMAN, R E (1977) "Analysis in Jointed Rocks", in Finite Elements in Geomechanics (ed G Gudehus), Wiley and Sons, 351-375.

GOODMAN, R E and ST JOHN, C (1977) "Finite Element Analysis for Discontinuous Rocks", Numerical Methods in Geotechnical Engineering, (ed C S Desai and J T Christian), McGraw Hill, 148-175.

HERRMANN, D A (1987) "Fracture Control in the Hangingwall and the Interaction between the Support system and the Overlying Strata", MSc Thesis, University of Witwatersrand.

HEUZE, F E and BARBOUR, T G (1982) "New Models for Rock Joints and Interfaces", J Geotech Eng Div, ASCE, 108, GT5, 757-776.

HEYMAN, J (1971) Plastic Design of Frames Vol 2: Applications, Cambridge University Press, London.

HEYMAN, J (1977) Equilibrium of Shell Structures, Oxford University Press, Oxford.

HIBBITT, KARLSSON, and SORENSEN (1987) "ABAQUS User's Manual".

HIBBITT, KARLSSON, and SORENSEN (1987) "ABAQUS Theory Manual".

JAEGER, J C and COOK, N G W (1969) Fundamentals of Rock Mechanics, Chaplan and Hall, London.

University of Cape Town

JOUGHIN, N C and JAGER, A J (1984) "Fracture of Rocks at Stope Faces in South African Gold Mines", Trans Inst Min Metall.

JUMIKUS, A R (1979) Rock Mechanics, Trans Tech.

LADANYI, B and ARCHAMBAULT, G (1970) "Simulation of Shear Behaviour of a Jointed Rock Mass", Proc 11th Symp Rock Mech, 105-125.

LEONTOVICH, V (1959) Frames and Arches, McGraw-Hill, London.

PENDER, M J (1985) "Prefailure Joint Dilatancy and the Behaviour of a Beam with Vertical Joints", Rock Mech and Rock Eng, 18, 253-266.

PLESHA, M E (1986) "Mixed Time Integration for the Transient Analysis of Jointed Media", Int J Num and Anal Methods in Geomech, 10, 91-110.

PLESHA, M E (1987) "Constitutive Models for Rock Discontinuities with Dilatancy and Surface Degradation", Int J Num and Anal Meth in Geomech, 11, 345-362.

ROBERDS, W J and EINSTEIN, H H (1978) "Comprehensive Model for Rock Discontinuities", J Geotech Eng Div, ASCE, 104, GT5, 553-569.

STAGG, K G and ZIENKIEWICZ, O C (1969) Rock Mechanics in Engineering Practice, Wiley and Sons.

TIMOSHENKO, S P and GERE, J M (1961) Theory of Elastic Stability, McGraw-Hill, London.

WILSON, E L (1977) "Finite Elements for Foundations, Joints and Fluids", in Finite Elements in Geomechanics (ed G Gudehus), Wiley and Sons, 319-350.

University of Cape Town

ZIENKIEWICZ, O C (1970) "Analysis of Nonlinear Problems with Particular Reference to Jointed Rock Systems", Proc 2nd Int Conf Society of Rock Mech, Belgrade, 3, 501-509.

ZIENKIEWICZ, O C (1971) The Finite Element Method in Engineering Science, McGraw-Hill, London.

University of Cape Town

APPENDIX

Courses completed in partial fulfilment of the M.Sc. Degree

Course		Date	Credits
CIV 525S	Contract Law	1987	3
CIV 540F	Finite Element Analysis	1987	4
CIV 588F	Applied Mechanics I	1987	3
CIV 589S	Applied Mechanics II	1987	3
AMA 363F	Numerical Analysis	1987	3
AMA 367F	Continuum Mechanics	1987	3
AMA 368S	Numerical Solution to Differential Equations	1987	3
		TOTAL	22

University of Cape Town

27 JUN 1989